Sonoporation: Applications for Cancer Therapy

15

Jiale Qin, Tzu-Yin Wang, and Jürgen K. Willmann

Abstract

Therapeutic efficacy of both traditional chemotherapy and gene therapy in cancer is highly dependent on the ability to deliver drugs across natural barriers, such as the vessel wall or tumor cell membranes. In this regard, sonoporation induced by ultrasound-guided microbubble (USMB) destruction has been widely investigated in the enhancement of therapeutic drug delivery given it can help overcome these natural barriers, thereby increasing drug delivery into cancer. In this chapter we discuss challenges in current cancer therapy and how some of these challenges could be overcome using USMB-mediated drug delivery. We particularly focus on recent advances in delivery approaches that have been developed to further improve therapeutic efficiency and specificity of various cancer treatments. An example of clinical translation of USMB-mediated drug delivery is also shown.

Keywords

Sonoporation • Drug delivery • Cancer

15.1 Introduction

Cancer has emerged as the leading cause of human death worldwide (Jemal et al. 2011). In 2012, approximately 14.1 million patients were diagnosed and about 8.2 million patients died from cancer (Ferlay et al. 2014). This high mortality primarily results from a lack of effective therapy in many cancer types. Current treatment approaches include either surgical removal with and without adjuvant radiation and/or systemic chemotherapy, primary radiation or chemotherapy (Minchinton and Tannock 2006; Jain 1998). However, most chemotherapeutics lack tumor specificity, leading to high systemic toxicity. In addition to chemotherapy, gene therapy has been investigated as an alternative treatment approach

J. Qin • T.-Y. Wang • J.K. Willmann (✉)
Department of Radiology,
Molecular Imaging Program at Stanford,
Stanford University, School of Medicine,
Stanford, CA, USA
e-mail: willmann@stanford.edu

J.-M. Escoffre, A. Bouakaz (eds.), *Therapeutic Ultrasound*, Advances in Experimental Medicine and Biology, Vol. 880, DOI 10.1007/978-3-319-22536-4_15

as it has demonstrated promising antitumor effects in preclinical studies. However, major hurdles still exist for this treatment approach in terms of safe methods to selectively deliver therapeutic genes into tumor cells and high enough gene expression levels to efficiently eradicate tumors *in-vivo* (Shillitoe 2009; Tong et al. 2009).

Over the last two decades, several methods have been developed to deliver drugs, including genes, to the tumor target location using an externally applied "trigger" (Waite and Roth 2012; Guarneri et al. 2012). Among these methods, ultrasound-guided microbubble (USMB) destruction has great potential for clinical translation in oncology because it is a safe, non-invasive, cost-effective and non-ionizing modality (Edelstein et al. 2007). Importantly, this approach can create temporary and reversible openings in vessel walls and cellular membranes through a process called "sonoporation", allowing enhanced transport of therapeutic agents across these biological barriers in the insonated region (Tzu-Yin et al. 2014; Kaneko and Willmann 2012).

An in-depth description of the mechanisms of sonoporation can be found in previous chapters of this book. Here, we focus on the *in-vitro* and *in-vivo* investigations on USMB-mediated drug delivery in various tumor models for improved cancer therapy. Specifically, we discuss how USMB assists in overcoming the challenges of drug delivery into tumors, general treatment protocols, current status in preclinical and clinical applications, as well as future directions for clinical translation of this technique.

15.2 Tumor Microenvironment and Pathways of Sonoporation-Mediated Drug Delivery

Although many anticancer agents are effective in killing monolayer tumor cells grown in culture, their treatment effects are significantly reduced *in-vivo* because the *in-vivo* tumor microenvironment creates several barriers for drug delivery into tumor cells (Lozano et al. 2012). Most solid tumors are composed of proliferating tumor cells, tumor stroma (including the extracellular matrix of tumors) and angiogenic vessels, which are different from normal tissues. The tumor vasculature is chaotic in terms of spatial distribution, microvessel length and diameter. Vessels are also tortuous and saccular, possessing haphazard interconnections (Wang and Yuan 2006) and they show leaky pores, allowing for larger particles up to a few hundred nanometers to pass through (Hobbs et al. 1998). Also, the tumor architecture generally lacks adequate lymphatic drainage. The combination of high vascular permeability and inadequate lymphatic drainage results in an increased interstitial fluid pressure, which severely limits convection-dependent transport of agents in the interstitium (Boucher et al. 1990). Furthermore, the extracellular matrix of tumors, a combination of proteoglycans, collagens and additional molecules (Mow et al. 1984), can limit interstitial transport and prevent sufficient and uniform distribution of anti-cancer agents (Wang and Yuan 2006). Finally, actively proliferating tumor cells can force the vessels apart, leading to an increased distance between the tumor cells and the blood vessels. The tumor cells can be separated from the blood vessels by more than 100 μm (Minchinton and Tannock 2006). Due to high interstitial fluid pressures, transport barriers in the extracellular matrix, and an increased distance from the vessels to the cells, usually only limited quantities of therapeutic agents reach tumor cells by diffusion only.

USMB-mediated drug delivery has been reported to result in a 20–80 % improvement in tumor response to drug treatment compared with administration of drugs alone in preclinical murine models (Yu et al. 2013; Sorace et al. 2012; Pu et al. 2014; Duvshani-Eshet et al. 2007; Carson et al. 2012). In an USMB delivery system, hydrophobic gas-filled microbubbles, stabilized by a lipid, protein or polymer shell, are exposed to ultrasound (Sirsi and Borden 2014). During exposure, the microbubbles can undergo volumetric change and/or violent collapse, a process called cavitation (Tzu-Yin et al. 2014). Cavitation can occur in two forms: stable and inertial. Stable cavitation occurs when the microbubbles oscillate stably around a resonant

diameter at low acoustic intensities. At higher intensities, the microbubbles undergo much more violent expansion, contraction and forcible collapse, generating shock waves in the vicinity of the microbubbles, a process called inertial cavitation (Newman and Bettinger 2007). Both forms of cavitation can create pores on the nearby cellular membranes (Matsuo et al. 2011; Zhang et al. 2012) and vessel walls (Bekeredjian et al. 2007; Bohmer et al. 2010), allowing for transport of particles. In addition, the fluid motion induced during the cavitation process may enhance the transportation of drugs into the interstitium, increasing the quantities of agents that can reach more distant tumor cells (Eggen et al. 2013).

While multiple novel treatment approaches are being explored, in this chapter we focus on two USMB-mediated drug delivery approaches currently being investigated for cancer therapy. The first approach aims to kill tumor parenchymal cells by delivering cytotoxic or cytostatic antitumor therapeutics across the vessel, through the interstitium, and into tumor cells, *i.e.*, a transvascular-interstitial-transmembrane pathway. The second approach aims to destroy tumor vasculature by either killing the vascular endothelial cells or mechanically destructing the tumor vasculature in order to compromise tumor blood supply. Both approaches are discussed in the following sections.

15.2.1 Tumor Treatment Through a Transvascular-Interstitial-Intracellular Pathway

The major challenge of drug delivery into tumor cells through this pathway is the need to push therapeutic agents across several barriers: (1) across vessels, (2) interstitial transport, and (3) passage into tumor cell.

15.2.1.1 Transvascular Transport by Modulating Vascular Integrity

Inertial cavitation of microbubbles in the lumen of tumor vessels may disrupt vascular endothelial integrity due to shock waves and jetting during collapse of microbubbles (Qin et al. 2009). On the other hand, stable cavitation is thought to temporarily increase the gap-junction distance between vascular endothelial cells by a volumetric change of the oscillating microbubbles. In the expansion phase, the large microbubbles may cause a circumferential displacement of the vessel, and the contraction phase may cause invagination of the interacted vessel (Chen et al. 2011; Caskey et al. 2007). Both forms of cavitation can lead to pores on the vessel wall, allowing for circulating therapeutic agents to extravasate across the vessels wall into the tumor interstitium (Fig. 15.1a).

Bekeredjian et al. (2007)) injected Evans blue dye (a highly charged low molecular weight marker that binds to serum albumin (about 69 kDa) to become a high molecular weight intravascular tracer protein) (Hoffmann et al. 2011; Elodie Debefve et al. 2013) and lipid microbubbles into hepatoma-bearing rats and insonated the tumors with ultrasound (1.3 MHz, mechanical index 1.6, bursting pulses every 4 cardiac cycles for 15 min). They showed an approximate five-fold higher Evans blue dye accumulation in insonated compared to non-insonated tumors. The amount of Evans blue extravasation has also been shown to be affected by both the microbubble type and the acoustic conditions. Bohmer et al. (2010)) showed that ultrasound (10,000 cycles of 1.2 MHz ultrasound pulsed at 2 MPa pressure and a pulsing rate of 0.25 Hz for 5 min) increased Evans blue extravasation by a factor of 2.3 in the presence of lipid-shelled mircobubbles, compared to a factor of 1.6 in the presence of polymer-shelled microbubbles in murine colon cancers subcutaneously established in mice. This difference likely occurred because the cavitation threshold is lower for lipid-shelled microbubbles. In the same study, two acoustic conditions were compared: Pulse lengths of 100 and 10,000 cycles. The results showed that the spatial extent of extravasation was significantly smaller for 100 cycles per pulse than for 10,000 cycles (6 ~ 9 mm vs. 18 ~ 20 mm), while other ultrasound parameters (1.2 MHz, 2 MPa pressure and pulsing rate of 0.25 Hz for 5 min) and the microbubble type (polymer-shelled microbubbles) were kept the same.

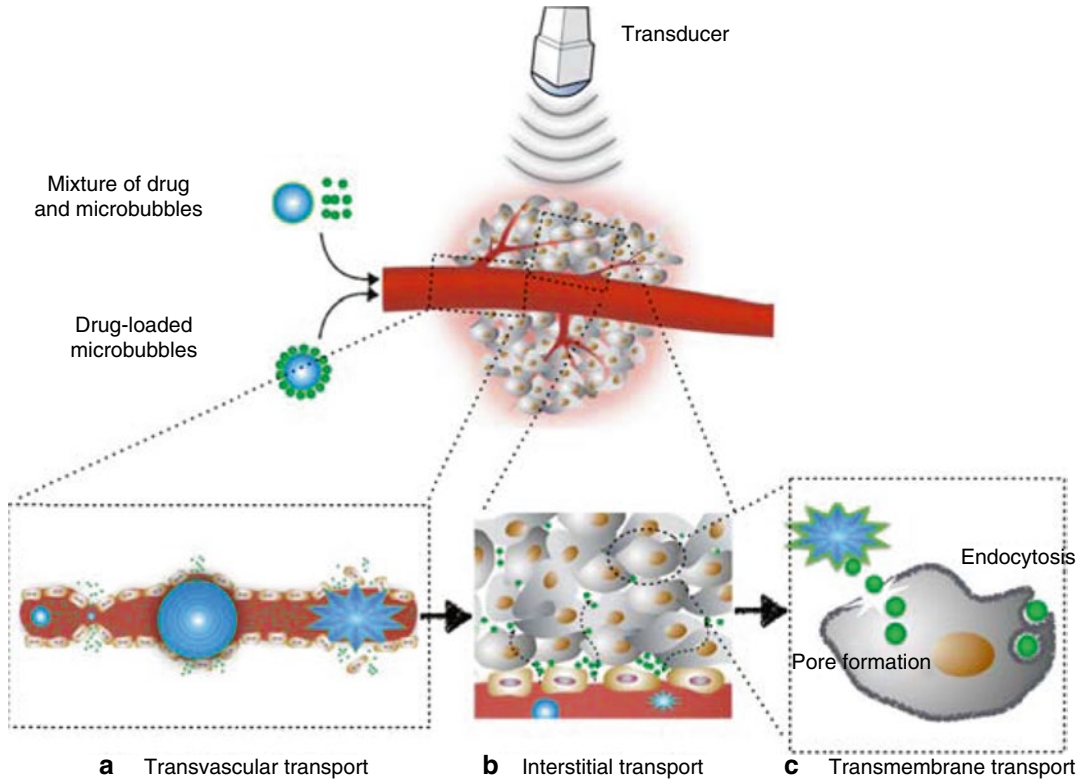

Fig. 15.1 Schematic summary of the transvascular-interstitial-transmembrane pathway in USMB-mediated drug delivery. (**a**) Potential mechanisms responsible for the passage across the vessels include creation of temporary gaps between vascular endothelial cells by volumetric expansion and contraction of the oscillating microbubbles. Also, cavitation of microbubbles may disrupt vascular endothelial cell integrity during violent collapse of microbubbles, creating ruptures in the vascular endothelial layer. (**b**) Interstitial transport of drugs/genes within the extracellular matrix may be enhanced by ultrasound radiation force. (**c**) USMB may induce membrane disruption and/or enhance active transport, such as endocytosis, thereby enhancing cellular permeability

Since Evans blue dye bound to serum albumin is relatively small (7 nm) (Elodie Debefve et al. 2013) compared to many therapeutic agents, another study assessed whether USMB can also increase tumor delivery of other model drugs that are larger in size. Carlisle et al. (2013)) demonstrated that USMB (ultrasound: 0.5 MHz, 50,000 cycles pulse length, 0.5 Hz pulse repetition frequency, 1.2 MPa peak rarefactional pressure for 4 min; SonoVue® microbubbles) increased extravasation and intratumoral (i.t.) distribution of a 130-nm luciferase labeled polymer-coated adenovirus in a breast cancer mouse model. Compared with non-insonated tumor, USMB resulted in a 5-fold increase in the amount of delivered adenovirus within 100 μm of blood vessels, and an increase of 40 fold beyond 100 μm. This suggests that USMB may not only increase the amount of drug extravasation, but also enhance drug penetration in the tumor interstitium, as shown in the following section.

15.2.1.2 Interstitial Transport

The high interstitial fluid pressure in tumors can reduce the convectional transport of drugs and particles throughout the extracellular matrix and, hence, only a small population of neoplastic cells located close to blood vessels is exposed to therapeutic agents by diffusion (Bae 2009; Davies Cde et al. 2004). Application of ultrasound has been shown to facilitate drug penetration beyond the close proximity of tumor vessels, potentially through radiation force caused by ultrasound (Fig. 15.1b). Radiation force is produced by the pressure gradient caused by a momentum transfer from the wave to the attenuating media, arising

either from absorption or reflection of the wave. This momentum transfer from ultrasound beam to a particle causes the transport of the particle in the direction of wave propagation. Due to higher tissue absorption at higher frequencies, the radiation force increases with increasing frequencies.

In a study performed by Eggen et al. (2013), prostate tumors established in mice were exposed to ultrasound (1 or 0.3 MHz, 13.35 W/cm^2, mechanical index 2.2, 5 % duty cycle, total exposure 10 min) 24 h after the administration of liposomes. At this time point, liposomes had passively extravasated into the tumor via the enhanced permeability and retention (EPR) effect, with a very low remaining concentration in the circulation (only approximately 10 % of liposomes in the circulation 24 h after injection). Since the blood liposome concentrations at 24 h was so low, changes of liposomal tumor distribution following ultrasound application was considered to be caused by its effect on already extravasated liposomes, rather than liposomes still in circulation. The study showed that liposomes in tumors insonated with ultrasound were more scattered throughout the tumor volume and penetrated two-fold more from blood vessels compared to those in non-insonated tumors. Moreover, the penetration distance was larger when the higher frequency (1 MHz) was applied. One potential explanation for this phenomenon is that the acoustic radiation force enhances drug transport. As the ultrasound frequency increased from 0.3 to 1 MHz, the radiation force could be increased, thus facilitating the transport of particles in the interstitium. This study demonstrated that radiation force from ultrasound may propel interstitial transport of extravasated therapeutic agents within the interstitial space. The increased penetration depth may allow the therapeutic agents to act on deeper lying tumor cells, eventually improving the outcome of tumor drug therapy.

However, the penetration depth of therapeutic agents varies at different spatial locations within tumors. Eggen et al. (2014) showed that USMB had a different impact on drug delivery in the periphery versus the core of tumors. In a prostatic cancer mouse model, USMB resulted in an increased nanoparticle penetration distance of 0.5–1 nm in the tumor periphery compared to the tumor core. This phenomenon was potentially caused by the heterogeneous distribution of interstitial fluid pressure across tumors. Indeed, in other studies using subcutaneous rat breast cancer models (Boucher et al. 1990) and a subcutaneous human osteosarcoma xenograft model (Eikenes et al. 2004), the interstitial fluid pressure rose with increased distance from the tumor periphery to the core within the first 400 μm, and then plateaued afterwards. The elevated interstitial fluid pressure may hinder transport of the extravasated particles in the interstitial space, resulting in shorter penetration in the tumor core.

15.2.1.3 Transmembrane Transport of Tumor Parenchymal Cells

The process of USMB-mediated permeability enhancement of tumor cells can be induced by pore formation and/or active transport across the membrane (Fig. 15.1c).

Pore formation in tumor cells has been visualized in many *in-vitro* studies, such as melanoma C32 cells (Matsuo et al. 2011) and prostate cancer DU145 cells (Zhang et al. 2012) by electron microscopy. Stable and inertial cavitations have been shown to cause cell membrane displacement and disruption for improved drug delivery across cellular membranes (Taniyama et al. 2002; van Wamel et al. 2004). Pore sizes between 100 nm and a few micrometers have been reported (Schlicher et al. 2006). This implies that exogenous antitumor agents with sizes smaller than the pore size could passively diffuse into the cytoplasm *in-vitro* via pores created by USMB. However, these observations were made in a simple *in-vitro* setting with monolayers of cells cultured in a fluid environment. It is not clear whether USMB also causes pore formation *in-vivo*, where tumor parenchymal cells are located in a densely packed solid tissue environment.

In addition to passive diffusion through nonspecific pores on tumor cell membranes, USMB has also been shown to assist in active drug transport mechanisms into the cytoplasm, such as endocytosis, especially for larger molecules (>500 kDa). Meijering et al. (2009) and Juffermans et al. (2014) demonstrated that cellular uptake of larger molecules relied on endocytosis alone; whereas cellular uptake of smaller

molecules involved both pore formation and endocytosis. Chuang et al. (2014) used microscopy to show the endocytotic process (24 h) by which albumin-shelled microbubbles loaded with paclitaxel (1.91 μm) enter breast cancer cells in presence of acoustic exposure, resulting in increased transport of albumin microbubbles into tumor cells. The exact mechanism behind USMB-induced endocytosis has not been completely elucidated. It has been speculated that ultrasound exposure and microbubble cavitation trigger changes in the membrane ion channels and the cytoskeletal arrangement, leading to an increase in intracellular Ca^{2+} (Parvizi et al. 2002) and polymerization of microtubules (Hauser et al. 2009). The changes may lead to enhanced endocytotic activity, thereby causing an increase in extracellular drug uptake in insonated cells. A detailed description on the microbubble-membrane interaction can be found in previous chapters of this book.

Indeed, the interaction between microbubbles and cells occurs within close proximity to the cells (Tzu-Yin et al. 2014). *In-vivo*, since microbubbles are spatially limited within the vessels, USMB induced in the vessel may only affect very few parenchymal cells near the vasculature (Ward et al. 2000). Therefore, successful drug delivery into distant parenchymal cells may require combination of USMB and other slow release therapeutic carrier systems. While USMB allows for passage of the therapeutic carriers across the vessels, the extravasated therapeutic carriers diffuse into the tumor parenchyma and slowly release the drug payload into tumor cells (Cochran et al. 2011a).

15.2.2 Destruction of Tumor Vascular

An alternative approach to cancer therapy is to destroy tumor vasculature by USMB. Exposure of tumor vessels to oscillating and imploding microbubbles can not only increase vascular endothelial cell membrane permeability, thereby enhancing uptake of anti-tumoral or anti-angiogenic in the vessels, but can also directly and mechanically destroy tumor vasculature. Both phenomena can cause blood vessel shut down with decreased supply of nutrients to tumor tissue (Molema et al. 1998).

15.2.2.1 Enhanced Cellular Uptake of Drugs in Vascular Endothelial Cells

The ultrasound-microbubble-cell interaction in the lumen of tumor vessels can selectively stimulate uptake of cytotoxic or anti-angiogenic drugs in vascular endothelial cells, leading to cellular apoptosis and subsequent disruption of the tumor vasculature (Fig. 15.2a).

In-vitro, this enhanced endothelial cellular uptake has been demonstrated using a dye, as well as fluorescently labeled molecules with difference sizes, such as propidium iodide (0.8 nm) (van Wamel et al. 2006), DiI (1 nm) (Patil et al. 2011), dextran (4.4 kDa) (Meijering et al. 2009), 5-carboxytetramethylrhodamine labeled small interfering RNA (siRNA about 15 kDa) (Juffermans et al. 2014), fluorescein isothiocyanate (FITC)-labeled dextran (500 kDa) (Taniyama et al. 2002) and Cy3-labeled plasmid DNA (about 3,500 kDa) (van Wamel et al. 2004). *In-vivo*, Fujii et al. (2013) demonstrated enhanced uptake of plasmid in endothelial cells in a heterotopic mammary adenocarcinoma model. In this study, vascular endothelial growth factor receptor-2 (VEGFR2) short hairpin (sh)RNA plasmid delivered by USMB (1.3 MHz, 0.9 W power, 10 s pulsing intervals for 20 min; cationic lipid-shelled microbubbles) resulted in increased knockdown of VEGFR2, as examined by PCR, immunostaining and western blotting. *In-vivo* contrast-enhanced ultrasound imaging further confirmed decreased tumor microvascular blood volume and blood flow in tumors treated with plasmid and USMB compared to tumors treated with plasmid alone.

15.2.2.2 Mechanical Destruction of the Tumor Vasculature

In addition to delivering anti-angiogenic therapeutics, USMB alone without adding therapeutic agents has been shown to have a direct anti-angiogenic effect in tumors (Fig. 15.2b). Wood et al. (2008) observed an acute shutdown of blood flow (as measured by Power Doppler) along with increased necrosis and apoptosis by histology following the administration of Definity® microbubbles and low intensity ultrasound (1 MHz at 2.2 $W.cm^{-2}$ or 3 MHz at 2.4 $W.cm^{-2}$; treatment for 3 min) in a murine melanoma model. Similarly, an acute

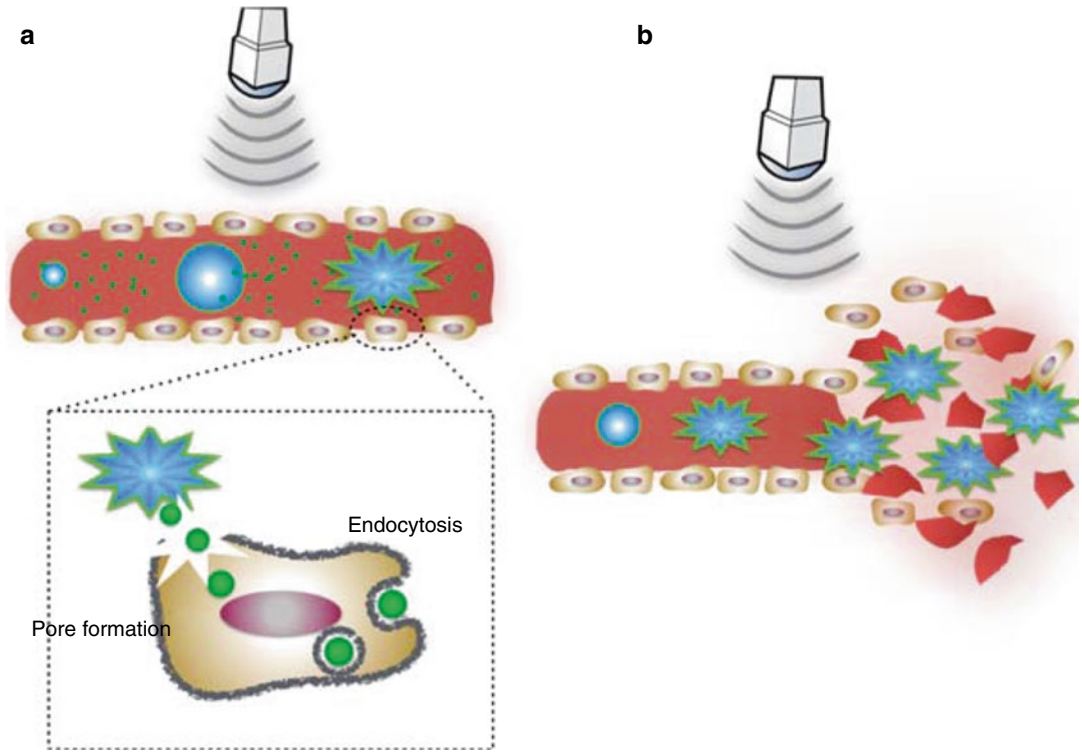

Fig. 15.2 Schematic drawing of destruction of tumor vasculature in USMB treatment. (**a**) Ultrasound-microbubble-cell interaction in the lumen of tumor vessels can stimulate uptake of cytotoxic or anti-angiogenic drugs in vascular endothelial cells by either creating pores on the cellular membrane and/or stimulating active transport, such as endocytosis. (**b**) USMB alone can directly produce an anti-angiogenic effect by mechanically disrupting tumor vasculature

decrease of blood flow by USMB alone (1 MHz, 0.1 ms pulse length, 1.6 MPa, Definity® microbubbles) was demonstrated in an *in-vivo* breast cancer model by Todorova et al. (2013). In this study, vessels in the tumor center were more preferentially disrupted versus those in the tumor periphery.

15.3 Treatment Protocols in Preclinical Experiments

USMB treatments require sufficient accumulation of microbubbles and drugs and appropriate ultrasound waves at the target tissues (Panje et al. 2012). The microbubbles and drugs can be delivered through different routes (intravenous (i.v.), intratumoral (i.t.) or intraperitoneal (i.p.)). The drugs can be mixed in the microbubble solution prior to administration or loaded on the microbubbles. Once the microbubbles and drugs reach the target tissues, appropriate ultrasound waves need to be delivered in a timely manner to produce optimal release of drugs (Willmann et al. 2008, Fig. 15.3).

In general, USMB treatment protocols involve systemic or local administration of microbubbles, along with a combination of therapeutic agents, followed by imaging-guided application of extracorporeal acoustic energy to actuate sonoporation at the desired delivery site. Delivery outcomes can be influenced by several factors, including but not limited to (1) whether drugs are mixed with or loaded on microbubbles, (2) routes of microbubble and drug administration, (3) ultrasound parameters, and (4) the temporal sequence of treatment. Several studies have investigated the influence of these factors on drug delivery efficiency in order to optimize treatment outcomes in cancer and to ultimately prepare this technique for clinical translation.

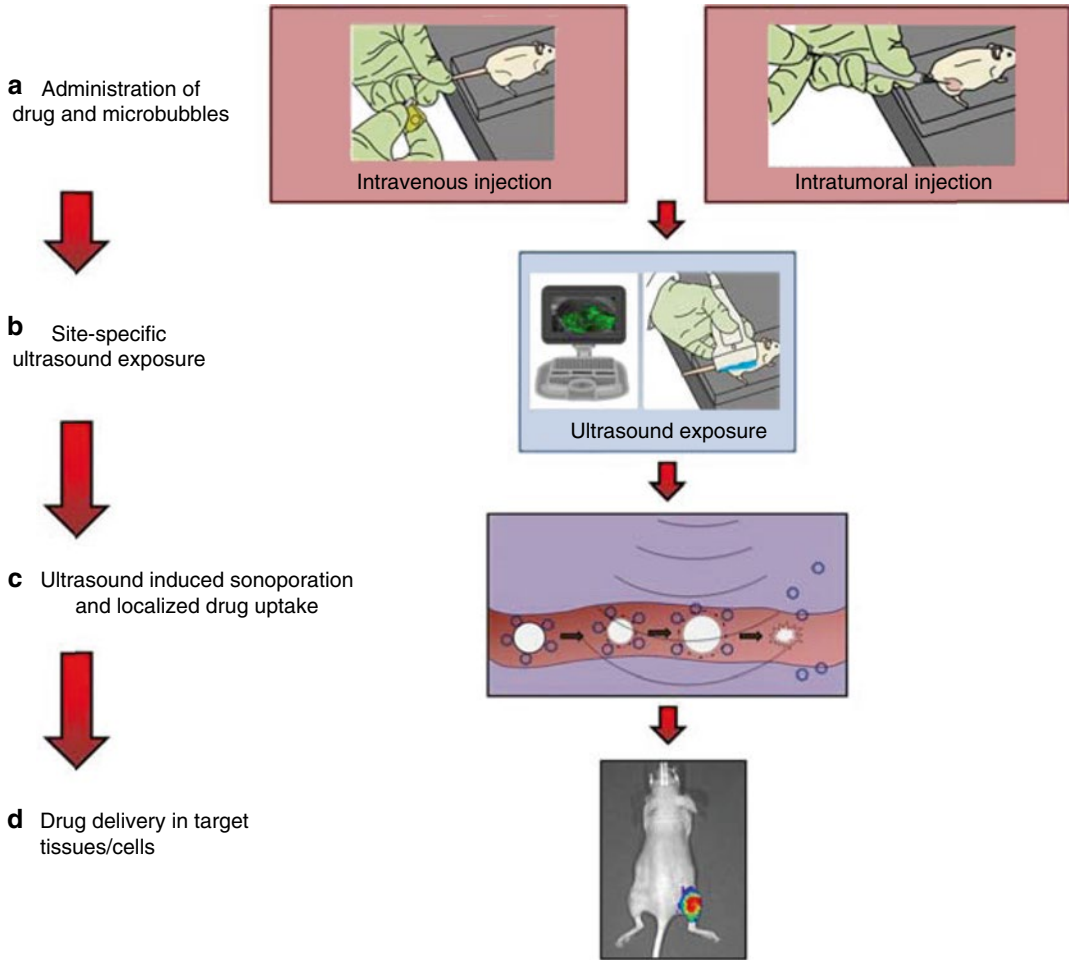

Fig. 15.3 Typical treatment protocol of USMB-mediated drug delivery in preclinical *in-vivo* experiments. (**a**) Microbubbles and therapeutic agents are administered either systemically via intravenous injection or locally through, for example, intratumoral injection. (**b**, **c**) Site-specific ultrasound exposure with the presence of microbubbles triggers sonoporation, facilitating the uptake of therapeutic agents. (**d**) Drug delivery outcomes could be quantified and monitored noninvasively using, for example, bioluminescence imaging shown here or other imaging modalities. Here, focal bioluminescent signal on the right hind limb of a mouse shows successful delivery of a reporter gene to the right hind limb tumor, while no imaging signal is observed elsewhere, demonstrating site-specific delivery limited to the region of insonation (This figure is adapted with permission from Panje et al. (2013))

15.3.1 Mixing Drugs with Microbubbles Versus Loading a Drug onto Microbubbles

15.3.1.1 Mixture of Drug and Microbubbles

One approach to USMB-mediated drug delivery is co-injecting a mixture of microbubbles and therapeutic agents. The advantage of this approach is the accessibility of already commercially available clinical grade microbubbles, such as Optison®, Definity® and Lumason®, all of which are FDA-approved for clinical contrast-enhanced ultrasound imaging. Sorace et al. (2012) intravenously injected Taxol, a chemotherapeutic for breast cancer, along with Definity® in breast cancer bearing xenografts in

mice followed by ultrasound insonation (1.0 MHz, 5 s pulse repetition period, mechanical index 0.5, 20 % duty cycle for 5 min). Over a 3-week treatment period, these tumors showed almost a 40 % increased inhibition and a higher degree of necrosis compared to the tumors treated with drugs alone. Wang et al. 2013a intravenously injected SonoVue® along with a suicide gene, herpes simplex virus-thymidine kinase gene (HSV-TK), for USMB treatment (mechanical index 1.2 for 10 min). They observed that USMB resulted in a 47-fold enhanced TK mRNA expression and a more than 2-fold apoptosis rate in an ovarian cancer model in mice. More examples (Sorace et al. 2012; Duvshani-Eshet et al. 2007; Matsuo et al. 2011; Carlisle et al. 2013; Wang et al. 2013a, b; Nie et al. 2008; Liao et al. 2012; Kotopoulis et al. 2014; Zhao et al. 2012; Suzuki et al. 2010; Yamaguchi et al. 2011; Heath et al. 2012; Iwanaga et al. 2007) are summarized in Table 15.1.

15.3.1.2 Drug-Loaded Microbubbles

The drawbacks of co-injecting drugs freely along with microbubbles are (1) faster degradation of certain drugs (nucleic acid (Zhou et al. 2010; Greco et al. 2010; Haag et al. 2006) and RNA (Carson et al. 2012)), and (2) potentially increased toxicity to other organs (other than liver and spleen in which microbubbles are usually cleared). To address these issues, microbubbles have been exploited as drug delivery vehicles as they are amenable for surface modification. Several strategies have been proposed for conjugating therapeutic agents onto or into microbubble carriers, which are further detailed in Chap. 11. For example, drugs can be embedded within the microbubble shell, dissolved in an oily layer between the gas core and the shell, or linked to the surface of the microbubbles. However, the drug loading capacity using these approaches is generally low. To improve this, alternative techniques coupling drug loaded liposomes or nanoparticles onto the microbubble shell have been reported (Wang et al. 2012; Sirsi SR and Borden MA (2014) State-of-the-art materials for ultrasound-triggered drug delivery. Advanced drug delivery reviews.

15.3.2 Routes of Microbubbles and Antitumor Agent Administration

Several drug administration routes have been explored including i.v., i.t., and i.p. injections. Direct i.t. and i.p. injection allow delivery of high local concentrations but are invasive.

15.3.2.1 Intravenous Injection

In most studies on USMB-mediated drug delivery for cancer therapy in preclinical animal models, microbubbles and drugs are administered intravenously. The potential drawbacks of this approach are the potential systemic toxicity and, in the case of gene delivery, the rapid degradation of the agent in the circulation. Both disadvantages can be overcome by either attaching drugs directly onto microbubbles or by loading them into nanoparticles.

Another potential drawback of systemic administration is that the delivery efficiency may be limited in hypovascularized tumors, such as pancreatic cancer (Fukumura and Jain 2007), because this route relies on sufficient tumoral vascularity for circulating microbubbles and drugs to float into target lesions.

15.3.2.2 Intratumoral Injection

Several early proof-of-concept animal studies have used this approach and demonstrated improved drug delivery after ultrasound exposure (Duvshani-Eshet et al. 2007; Iwanaga et al. 2007; Haag et al. 2006). The main advantage of i.t. injection is the ability to deliver high concentrations of drugs directly to the site of desired treatment while minimizing systemic toxicity (Duvshani-Eshet et al. 2007). However, this method of administration is invasive and can be challenging if the target lesion is located in an area that is difficult to access.

15.3.2.3 Intraperitoneal Injection

This approach may be useful for primary peritoneal cancers or cancers with i.p. spread as local drug concentration can be increased at the tumor sites (Pu et al. 2014; Kotopoulis et al. 2014). It has been shown that i.p. injection of drugs can

Table 15.1 Examples of animals studies using ultrasound and microbubbles to deliver drugs/genes for cancer therapy

Cancer types	References	Animal models	Drugs	MBs	Techniques	Routes	Treatment outcomes
HCC	Cochran et al. (2011b)	sc 3924a rats	DOX	Drug-loaded polymer MBs	1 MHz, MI 0.4–0.45, 20 min	i.v., MBs, single	Drug concentration in liver tumors was increased by 7-fold compared to administration of free DOX, while drug concentrations in plasma and myocardium were reduced to 1/5 and 1/2, respectively.
	Nie et al. (2008)	sc Hepa1-6 mice	HSV-TK pDNA GCV	SonoVue®	1 MHz, 50 % DC, 2 W/cm^2, 5 min	i.v., MBs, pDNA i.p. GCV daily for 10 days	Tumor volume was approximately 1/2 of control group treated with TK and MBs at day 28. MST was significantly longer than control (survival ratio at day 100 was 50 % vs. 0 %)
	Zhou et al. (2010)	sc H22 mice	HSV-TK pDNA GCV	pDNA-loaded lipids MBs	1 MHz, 2 W/cm^2, 5 min	i.v., MBs, pDNA i.p. GCV daily for 14 days	Tumor growth was further inhibited by 37 % compared to HSV-TK pDNA alone. Longer MST and better life quality in an 80-day continuous observation period.
	Yu et al. (2013)	sc HepG2 mice	HSV-TK pDNA Timp3 pDNA	Liposomes MBs	1.3 MHz, MI 1.3, 1 s interval time for 5 min	i.v., MBs, pDNA i.p. GCV daily for 4 days	Tumor growth was further inhibited by 30 % in treatment with both pDNA and USMB compared to treatments with single gene under the same USMB settings.
PC	Kotopoulis et al. (2014)	Orthotopic MIA PaCa-2 mice	Gemcitabine	SonoVue®	1 MHz, MI 0.2, 40 % DC, 10 min	i.v., MBs i.p. Gemcitabine weekly for 8 wks	The primacy tumor presented only 1/3 size of those treated with drug alone. A slower onset of metastatic development was observed.

HCC LC Glioma	Liao et al. (2012)	sc/orthotopic BNL mice Orthotopic LL/2 mice Orthotopic RT-2 mice	Endostatin Calreticulin pDNA polytreated with DOX, GM-CSF or IL-12	SonoVue®	1 MHz, 0.4 W/cm^2, 20 % DC, 200 Hz PRF	i.m., MBs, pDNA, intermittent (weekly for 4 wks) or consecutive (daily for the initial 4 days) i.p. DOX twice i.t. GM-CSF & IL-12 single	Tumors significantly regressed in all groups. Intermittent regimen was much more effective than consecutive regimen. Administration of multiple therapeutic agents resulted in better treatment outcome than administration of single agent.
BC	Sorace et al. (2012)	sc 2LMP mice	PTX	Definity®	1 MHz, 5 s PRP, 20 % DC, 5 min, MI 0.1, 0.5, 1 or 2	i.v., MBs, PTX twice a wk for 3 wks	All 4 pressure levels resulted in decreased tumor growth. Among them, MI of 0.5 resulted in the highest percentage of necrosis.
	Yan et al. (2013)	sc 4 T1 mice	PTX	Drug-loaded liposomes MBs	2.25 MHz, 1 % DC 1 Hz PRF, 10 ms BL, 1.9 MPa, 10 min	i.v., MBs, 3 more times at 3-day intervals	Drug accumulation was 3.54- or 4.31- fold higher in tumors compared to the groups without MBs or ultrasound, while the accumulation was lower in liver & kidney.
	Zhao et al. (2012)	sc MDA-MB-435 mice	Liposomal-DOX	Lipids MBs	1 MHz, 0.3 W/cm^2 50 % DC, 10 s	i.v., MBs, drug every 2 days	Tumor growth was inhibited using either of the three treatment schedules (USMB applied 2 h before, 2 h after, or simultaneously with drug administration), although the effect in the group treated with USMB applied 2 h after drug administration was inferior to the others.

(continued)

Table 15.1 (continued)

Cancer types	References	Animal models	Drugs	MBs	Techniques	Routes	Treatment outcomes
BC	Carlisle et al. (2013)	sc ZR75-1 mice	Oncolytic adenovirus (polymer)	SonoVue®	0.5 MHz, 50,000 cycles/pulse length, 0.5 Hz PRF, 1.2 MPa, 4 min	i.v., MBs & polymer, single	Circulation half-life of oncolytic adenovirus was improved by more than 50-fold. Tumor infection was enhanced by more than 30-fold, resulting in improved tumor growth retardation and prolonged MST.
OC	Suzuki et al. (2010)	sc OV-HM mice	IL-12 pDNA	Liposome MBs	1 MHz, 0.7 W/cm^2, 1 min	i.t., MBs, pDNA single & 12-day repetitive treatments	Tumor growth was suppressed in both treatments. Complete tumor regression in 80 % of mice receiving repetitive treatments.
	Pu et al. (2014)	Orthotopic A2780/DDP mice	PTX	LHRHa-targeted drug-loaded MBs	0.3 MHz, 1 W/cm^2 50 % DC, 3 min	i.p., MBs every 3 days for 15 days	Tumor cell apoptosis increased by 38 %, angiogenesis reduced by 39 % in comparison to the non-targeted PTX-loaded MBs + US group.

Prostatic Cancer	Goertz et al. (2012)	sc PC3 mice	Docetaxel	Polymer MBs	1 MHz, 50 ms burst, 1.65 MPa, 3 min	i.v., MBs & drug, single & 4-week repetitive treatment	Compared to drug alone, single treatment of USMB and drug induced a four-fold increase in necrosis, and repetitive treatment delayed tumor growth with prolonged doubling time from 0.1 to 6.9 weeks.
	Duvshani-Eshet et al. (2007)	sc PC2 mice	Hemopexin-like domain fragment pDNA	Optison®	1 MHz, 2 W/cm^2, 30 % DC 20 min	i.t., MBs, pDNA single & 4-wk repetitive treatments	Tumor growth was inhibited by 50 % after single treatment and by 80 % after repetitive treatments.
	Greco et al. (2010)	sc DU-145 DU-Bcl-xL mice	Cancer terminator virus	Virus-loaded targeson	MI 0.7 m 1.8 MPa, 10 min	i.v., MBs weekly for 4 weeks	Primary and metastatic tumors and therapy-resistant tumors were completely eradicated. No tumor regrowth occurred 3 months after cessation of the therapy.
	Haag et al. (2006)	sc LNCaPbl mice	Androgen receptor AO	AO-loaded lipid MBs	1.5, 2.5 or 7 MHz, MI 1.9, 9 min	i.t., & i.v., MBs single	Stronger gene uptake in tumor tissue was detected after gene-loaded MB injection and ultrasound compared to MB complex alone (16~49 % vs. 2~18 %).

(continued)

Table 15.1 (continued)

Cancer types	References	Animal models	Drugs	MBs	Techniques	Routes	Treatment outcomes
Melanoma	Matsuo et al. (2011)	sc C32 mice	Melphalan	Sonazoid®	1.011 MHz, 0.064 W/cm^2, 0.5 Hz burst rate, 50 % DC, 2 min	i.t., MBs, drug. Every 2 days for 2 weeks	Tumor growth ratio was significantly reduced by nearly 2.5 fold compared to drug alone.
	Yamaguchi et al. (2011)	sc C32 mice	IFN-β pDNA	Sonazoid®	1.011 MHz, 0.22 W/cm^2, 50 % DC, 3 min	i.t., MBs, pDNA, weekly for 4 weeks	Tumor growth ratio was significantly reduced by 2-fold and nearly 1.5-fold compared to blank control and gene alone, respectively.
SCC	Heath et al. (2012)	sc SCC-5 mice	Cisplatin Cetuximab	Definity®	1 MHz, MI 0.5, 5 s PRP, 20 % DC, 5 min	i.v., MBs & drugs, twice weekly for 4 weeks	Tumors treated with USMB and drug exhibited a 21 ~ 26 % decrease in tumor size compared with drug alone.
	Iwanaga et al. (2007)	sc Ca9-22 mice	Bleomycin Cdt-B pDNA	Optison®	1 MHz, 2 W/cm^2, 50 % DC	i.t., MBs, pDNA. Every 2 days in the first and third wks	Tumor was completely suppressed at the end of experimental period (56 days) in the group of cdtB pDNA and USMB, and nearly disappeared in bleomycin and USMB.
	Carson et al. (2012)	sc SCC-VII mice	EGFR-siRNA	Gene-loaded lipids MBs	1.3 MHz, MI 1.6, 30 min	i.v., MBs, 3 times	EGFR knockdown was distributed widely (80 %) throughout treated tumors. Tumor doubling time was prolonged from 2.7 to 8.5 days compared to gene alone.

Glioma	Liu et al. (2010)	Orthotopic C6 rats	Carmustine	SonoVue®	0.4 MHz, 0.62 MPa, 10 ms burst length, 1 Hz PRF, 30 s	i.v., MBs & drug, single	Drug delivery was enhanced by two-fold. Tumor growth was inhibited. MST was prolonged from 33 to 53 days compared to drug alone.
	Treat et al. (2012)	Orthotopic 9 L rats	Liposomal-DOX	Definity®	1.7 MHz, 1.2 MPa, 10 ms burst length, 1 Hz PRF for 1–2 min repeated every 5 min	i.t., MBs, drug, single	Tumor doubling time was prolonged from 2.7 days to 3.7 days compared to drug alone. MST was improved.
	Ting et al. (2012)	Orthotopic C6 rats	Carmustine	Drug-loaded MBs	0.7 MPa, 10 ms burst length, 5 % DC, 5 Hz PRF, 1 min	i.v., MBs, twice	Circulation drug half-life was prolonged by four-fold. Drug accumulation in the liver was reduced fivefold compared to drug alone. Tumor growth ratio was significantly reduced from 117.4 to 39.6 % and MST was improved from 29.5 to 32.5 days compared to drug alone.

PC pancreatic cancer, *Wks* weeks, *LC* lung cancer, *BC* breast cancer, *PTX* paclitaxel, *BL* burst length, *LNCaPbl* androgen hypersensitive LNCaP subline, *AO* antisense oligonucleotide, *IFN*-β interferon-β, *SCC* squamous cell carcinoma, *Cdt-B* Cytolethal distending toxin B, *HCC* hepatocellular cancer, *MBs* microbubbles, *DOX* doxorubicin, *DC* duty cycle, *MI* mechanical index, *PRF* pulse repetition frequency, *PRP* pulse repetition period, *i.v.* intravenous, *i.t.* intratumoral, *i.p.* intreperitoneal, *i.m.* intramuscular, *HSV-TK/GCV* herpes simplex thymidine kinase gene/ganciclovir, *LHRH-R* luteinizing hormone-resealing hormone receptor, *TIMP3* tissue inhibitor of metalloproteinase 3, *GM-CSF* granulocyte-macrophage colony-stimulating factor, *IL-12* interleukin-12, *pDNA* plasmid DNA, *MST* mean survival time

result in 20- to 1,000-fold higher peritoneal drug concentrations compared to plasma concentrations (Zimm et al. 1987; Markman et al. 1992). Micron-sized microbubbles, injected intraperitoneally, can stably persist in the peritoneal cavity without rapid clearance through the lymphatic drainage (Pu et al. 2014; Kohane et al. 2006; Tsai et al. 2007). Recently, in a mouse model of metastatic peritoneal lesions of ovarian cancer, Pu et al. (2014) injected luteinizing hormone-releasing hormone (LHRH) receptor-targeted paclitaxel-loaded microbubbles into the mouse peritoneal cavity and exposed the abdomen to ultrasound for sonporation. These microbubbles specifically bind to tumor cells expressing LHRH, and upon exposure to ultrasound, encapsulated drugs can be locally released at the tumor sites. Compared to treatment with paclitaxel alone, this approach resulted in an approximately two-fold higher apoptosis rate, an extended median survival time of treated mice from 37 to 47 days, and an approximately 55 % reduced tumor angiogenesis. In patients, however, peritoneal spread of cancer is usually diffuse and further studies are needed to assess clinical practicability of this approach to efficiently treat a diffuse disease process, such as peritoneal carcinomatosis using USMB.

15.3.3 Ultrasound Parameters

Most studies have shown successful USMB-guided drug delivery using already available clinical ultrasound imaging systems; however, the reported delivery efficiency is inconsistent (Newman and Bettinger 2007), likely due to there being so far no standardization of the acoustic parameters. To date, standardized ultrasound parameters for drug delivery have not been determined on any of the current clinical ultrasound systems, possibly because the systems have limited tunable acoustic parameters. This makes it difficult to perform a systematic and parametric study for optimal drug delivery on these systems. Optimizing ultrasound parameters tailored for the purpose of drug delivery has the potential to improve treatment outcomes (Yu et al. 2013). To determine an optimal setting for effective delivery, some studies compared drug delivery outcomes using custom-built ultrasound systems with more flexibility in the acoustic parameters. A wider range of ultrasound parameters was tested in drug delivery into cells *in-vitro* (Sonoda et al. 2007; Ghoshal et al. 2012) and *in-vivo* (Sorace et al. 2012; Wang et al. 2013a, Haag et al. 2006). So far, standard ultrasound parameters for USMB drug delivery have not been established. *In-vivo* ultrasound settings suggested by current literature are as follows:

Ultrasound frequency: 0.4 ~ 3 MHz. Lower frequencies are more preferable in general because the pressure threshold to initiate cavitation is reduced in the low frequency range (Apfel and Holland 1991).

Ultrasound intensities: 0.3 ~ 3 W/cm^2. This range lies close to or above the level used in diagnostic ultrasound (0.1–100 mW/cm^2), but below that of high-intensity focused ultrasound (Dubinsky et al. 2008; Leslie and Kennedy 2006). This allows for drug delivery into tumors while minimizing damage to normal tissues.

Mechanical index: 0.2 ~ 1.9. Mechanical index is defined as the ratio of peak negative pressure in MPa and the square root of center frequency in MHz. This index indicates the likelihood of cavitation generation. The likelihood of cavitation increases with increasing ultrasound intensity and decreasing frequency, and the mechanical index of an acoustic field is used as a safety gauge on clinical ultrasound imaging systems. The FDA stipulated limitation of mechanical index for clinical diagnosis is 1.9. It is thought that cavitation is unlikely to occur at a mechanical index of less than 0.7 (Newman and Bettinger 2007). However, the presence of microbubbles in the acoustic field significantly reduces this threshold by a rather unpredictable degree. This allows for USMB-enhanced drug delivery under a mechanical index lower than 1.9 (Newman and Bettinger 2007).

Duty cycles: <1–90 %. Duty cycle specifies the percentage of time pulsed ultrasound transmission occurs (O'Brien 2007). Applied duty

cycles vary substantially among various publications and usually depend on the ultrasound intensity used. In general, long duty cycles combined with high intensities can cause thermal damage to tissues. To avoid unnecessary thermal effects, duty cycles are kept low when high intensities are used and vice versa.

Duration of ultrasound exposure: 10 s ~ 30 min. The exposure duration needs to be sufficiently long for complete destruction of the administered microbubbles. However, for safety reasons, the exposure duration should be shortened to the minimally required time to avoid excess tissue damage. Most investigators apply ultrasound for a period of 1–5 min.

15.3.4 Treatment Schedule

The treatment schedule, including the temporal sequence of drug administration, USMB treatment, and the length and interval durations of repeated treatment cycles can have substantial effects on treatment efficiency.

Given that USMB only increases the permeability for a few seconds to a few hours (Tzu-Yin et al. 2014; Fan et al. 2012; Sheikov et al. 2008; Park et al. 2012a), administration of therapeutic agents at different time points following USMB treatment could result in substantially different treatment outcomes, as recently demonstrated in an *in-vivo* model by Zhao et al. (2012). In their experiment, three different treatment schedules (USMB applied 2 h before, 2 h after, or simultaneously with the injection of doxorubicin-loaded liposomes) were tested in a human breast cancer model in mice. Tumor suppression was smallest in mice treated with USMB applied 2 h after drug administration, and comparable in the other two treatment groups. This indicates a lingering therapeutic window for drug delivery of at least 2 h after USMB. Knowing the therapeutic window after a certain USMB treatment is critical to maximize therapeutics in cancer.

The influence of treatment interval length on USMB therapeutic outcomes was further assessed by Liao et al. (2012). Two different USMB treatment schedules, combined with the administration of anti-angiogenic gene therapy using endostatin and calreticulin, were evaluated in a subcutaneous hepatocellular cancer model in mice. In the first group of animals, USMB was applied once a week over 4 weeks. In the second group, USMB was applied daily over the first 4 days and all tumors were observed over a 4-week period. Therapeutic effects were more pronounced in the first group compared to the second one, suggesting that a continuous systemic concentration of angiogenesis inhibitors administrated weekly may be more effective in tumor growth inhibition than the administration of a high dose during a short time period (Grossman et al. 2011; Kisker et al. 2001).

It is expected that in the future optimized treatment schedules may need to be assessed for different tumor types and different therapeutic agents to enable maximum treatment effects.

15.4 Application in Cancer Therapies

Numerous studies have shown successful USMB-mediated drug delivery to a number of different cancer types (Table 15.1). This technique has shown enhanced systemic chemotherapy tumoricidal effects, improved biodistribution with preferential local accumulation in tumor tissue, and reversal of drug resistance of certain cancer types. It has also been proposed as an adjuvant treatment to other cancer therapies, as well as a potential approach to cancer vaccination. In the following section, the current status of USMB-mediated drug delivery in different types of cancer therapies *in-vitro* and in preclinical animal models is reviewed.

15.4.1 Cancer Therapy

15.4.1.1 Enhanced Tumoricidal Effects

Multiple *in-vitro* and *in-vivo* studies have demonstrated that USMB improves tumoricidal effects, as evidenced by a reduction of tumor growth, increase in tumor apoptosis and necrosis,

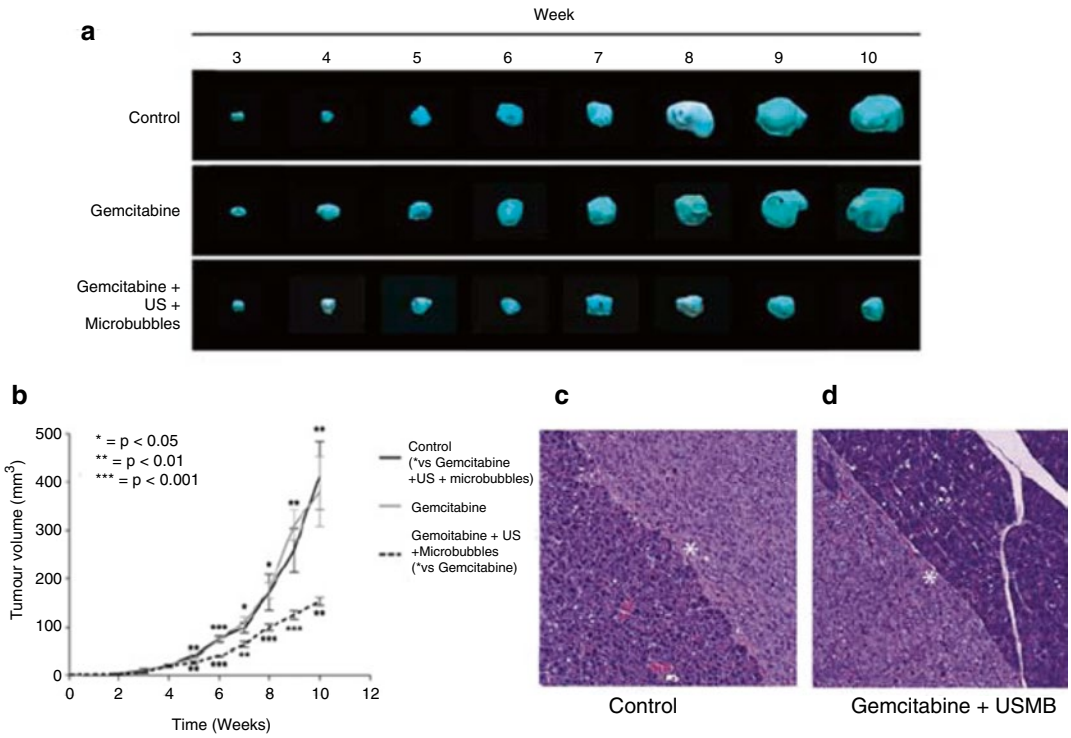

Fig. 15.4 Enhanced tumoricidal effect of USMB-mediated gemcitabine delivery in orthotopic pancreatic tumors in mice. (**a**) Compared to mice receiving weekly treatment of gemcitabine alone or no treatment (control), mice treated with USMB and gemcitabine presented a significantly suppressed tumor growth, as visualized in 3D tumor volumetric ultrasound images over time. (**b**) A statistically significant difference can be seen between the combined treatment group and the gemcitabine alone and/or control group after two treatment cycles. Histology images show a more invasive border between normal and tumor tissue in the control group (**c**), and a less invasive border in the gemcitabine and USMB group (**d**) (as indicated by the *asterisks*) (This figure is adapted with permission from Kotopoulis et al. (2014))

decrease in angiogenesis and regulation of relative protein expressions (Fig. 15.4).

For example, in a prostate tumor bearing mouse model (Goertz et al. 2012), intravenous injection of the chemotherapeutic docetaxel, along with microbubbles and ultrasound treatment, resulted in four-fold increase in necrosis compared to treatment with docetaxel alone at 24 h. In a mouse ovarian cancer model, Xing et al. (2008) investigated the level of tumor suppressor p53 after treatment with paclitaxel-loaded microbubbles and ultrasound. They showed that p53 expression was down-regulated 33 % more than in the paclitaxel alone group. Greco et al. (2010) treated mice with prostate cancer xenografts using USMB-assisted delivery of cancer terminator virus (CTV) with CTV-loaded microbubbles. They showed complete tumor response with complete tumor eradication following several weeks of weekly treatment. Even when animals were followed up to 3 months after the treatment, there was no tumor recurrence or metastatic spread in any of the mice. Similar complete response results were also reported in other murine cancer models, including head and neck squamous cell carcinoma (2007) and ovarian cancer (Greco et al. 2010).

Delivery of multiple medications, or polytherapy, using USMB can further enhance tumoricidal effects. Yu et al. (2013) administered a mixture of two therapeutic plasmids, HSV-TK/GCV and the tissue inhibitor of metalloproteinase 3 (Timp3), along with cationic microbubbles into mice bearing subcutaneous hepatocellular carcinomas and insonated the tumors with ultrasound. An additional 30 % improvement of tumor suppression was

observed compared with USMB-mediated delivery of either gene alone. Liao et al. (2012) treated orthotropic liver tumors in mice using USMB-assisted delivery of a combination of endostation (an anti-angiogenic gene) and interleukin-12 (an immunotherapeutic drug that prompts the immune system to fight cancer). The treatment resulted in an average tumor volume reduction to 7 % of the original size, while USMB-assisted delivery of either endostation or interleukin-12 alone resulted in a tumor volume reduction to only 52 % and 56 %, respectively.

Tumoricidal effects were observed not only in primary tumors but also in their metastases. Park et al. (2012b) studied treatment of breast cancer brain metastasis using USMB. A chemotherapeutic, trastuzumab, was co-injected along with Definity® microbubbles, and brain metastatic lesions were insonated by transcranial ultrasound. In animals treated with USMB and trastuzumab, an overall longer survival time, significant tumor suppression and even complete remission in some cases were observed compared to animals treated with intravenously injected trastuzumab alone. Pu et al. (2014) developed a method for treating metastatic ovarian cancer peritoneal lesions using the complex of LHRHa-targeted paclitaxel-loaded microbubbles. Five consecutive treatments with i.p. injection of this complex, followed by ultrasound exposure to the abdomen, resulted in approximately two-fold more cell apoptosis and 50 % lower microvessel density in peritoneal implants compared to the treatment with i.p. injection of paclitaxel alone.

In summary, USMB has demonstrated benefits in improving outcomes of many anti-cancer therapeutics in various preclinical tumor models, resulting in significantly increased tumoricidal effects, even complete remission in some cases.

15.4.1.2 Reduction of Toxicity of Chemotherapeutics

One of the most notorious problems of chemotherapy is its significant systemic toxicity, including cardiotoxicity and myelosuppression (Rahman et al. 2007). This issue could be addressed by the aforementioned technique of drug-loaded microbubbles with a spatially confined release of the encapsulated drug in the region exposed to ultrasound, while the drug remains on the microbubbles or nanoparticles, and rapidly clears before free drug exposes healthy tissues. For example, Cochran et al. (2011b) demonstrated preferential drug accumulation in the tumor, and smaller levels in normal organs, using doxorubicin-loaded microbubbles and ultrasound in a subcutaneous hepatoma mouse model. Specifically, the drug concentration was eight-fold higher in hepatoma (2.491 vs. 0.373 %/g tissue) and 50 % lower in the myocardium (0.168 vs. 0.320 %/g tissue) in mice treated with doxorubicin-loaded microbubbles, with ultrasound relative to the mice treated with the same dose of free drug (Fig. 15.5). Similar results were reported by Yan et al. (2013) in mice bearing breast cancer xenografts treated with paclitaxel liposome-loaded microbubbles and ultrasound. In tumors, a 3.5-fold higher paclitaxel tumor concentration could be obtained, along with significantly reduced levels of paclitaxel in normal liver and kidney tissues, compared to mice treated by free paclitaxel liposomes and ultrasound without microbubbles.

The lower drug concentration in the non-insonated healthy organ might reduce the toxicity of chemotherapeutics. Additionally, the preferential accumulation in insonated tumors suggests that the systemically administered dose may be reduced and yet still produce a comparable treatment effect in the diseased tissues. This may reduce the drug deposition in healthy organs, thus reducing the systemic toxicity. This feature has significant clinical implications in that it may reduce the systemic side effects in patients, as well as the financial burden of the cost of expensive chemotherapy drugs.

15.4.1.3 Reversal of Drug Resistance

Drug resistance is a common chemotherapy challenge resulting in failure of successful therapy in many cancers. For example, 75 % of pancreatic cancer patients are resistant to gemcitabine, even though it is the first-line chemotherapeutic agent for pancreatic adenocarcinoma (Ducreux et al. 1998). In breast cancer, only 60–70 % patients respond to anthracycline-based chemotherapy,

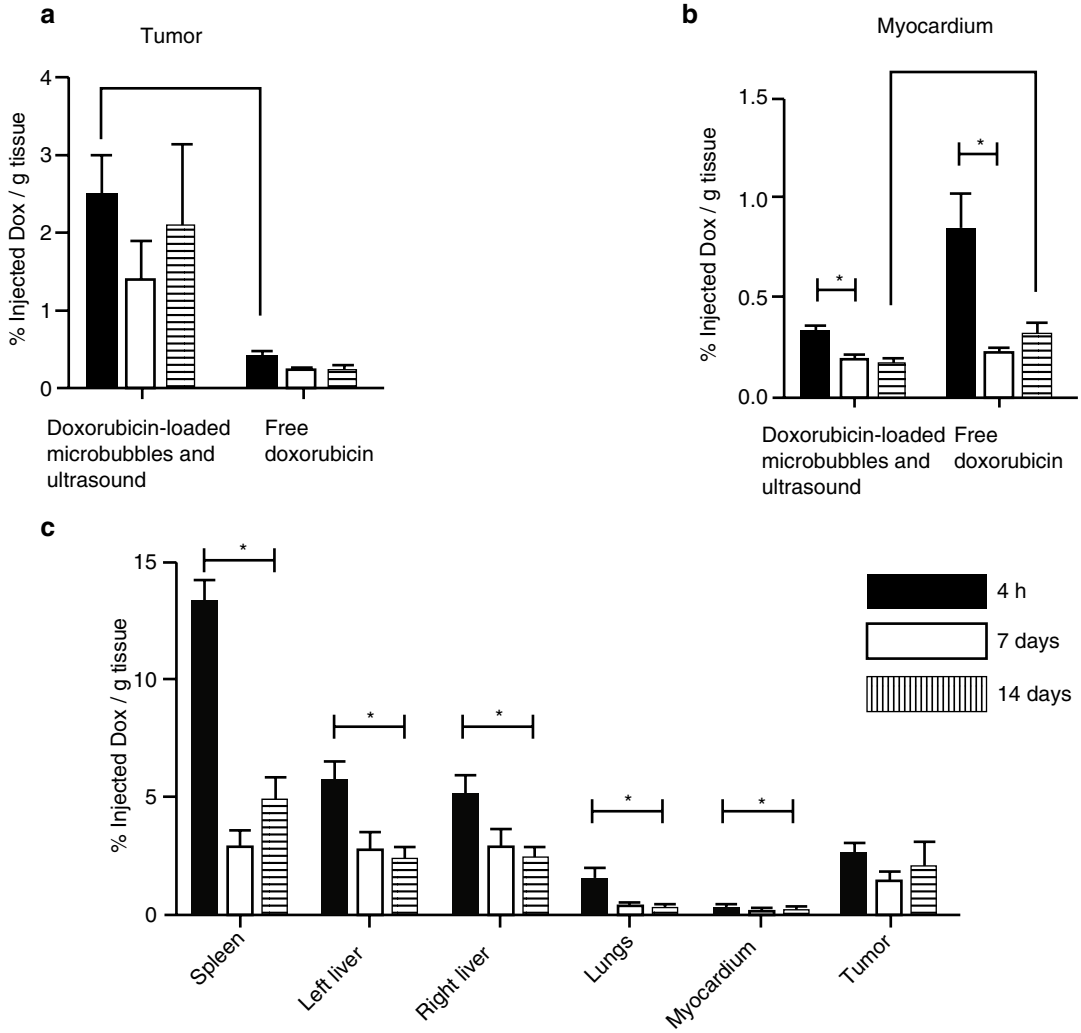

Fig. 15.5 Temporal and spatial distribution of doxorubicin in subcutaneous hepatoma-bearing mice treated with doxorubicin-loaded microbubbles and ultrasound or free doxorubicin alone. Compared to tumors treated with free doxorubicin, the treatment of doxorubicin-loaded microbubbles and ultrasound resulted in a higher doxorubicin concentration in the tumors (**a**) and lower concentrations in the myocardium (**b**). Doxorubicin levels in the spleen, liver, lungs, and myocardium all peaked at 4 h and dropped significantly after 14 days, whereas those in the tumor showed no significant drop from day 0 to day 14 (**c**). *$p<0.05$ (This figure is adapted with permission from Cochran et al. (2011b)

with only 14 % of them being completely responsive (Carey et al. 2006).

Drug resistance is often caused by the up-regulation of special transporters across the cancer cell membranes, preventing cellular uptake of drugs and/or ejecting drugs from the cytoplasm. An example is the multidrug resistance associated protein pumps, also known as P-glycoproteins, which are exporters of ATP-binding cassette transporters (Gottesman 2002; Szakacs et al. 2006).

Deng et al. (2013) observed that the use of USMB could help reduce drug resistance by down-regulating the level of P-glycoprotein in breast cancer cells *in-vitro*. Doxorubicin-resistant MCF-7 breast cancer cells were exposed to doxorubicin-liposome-microbubble complexes and insonated by ultrasound. Cells treated with doxorubicin-liposome-microbubble complex and ultrasound showed a more rapid cellular uptake, enhanced nuclear accumulation of drugs, and less

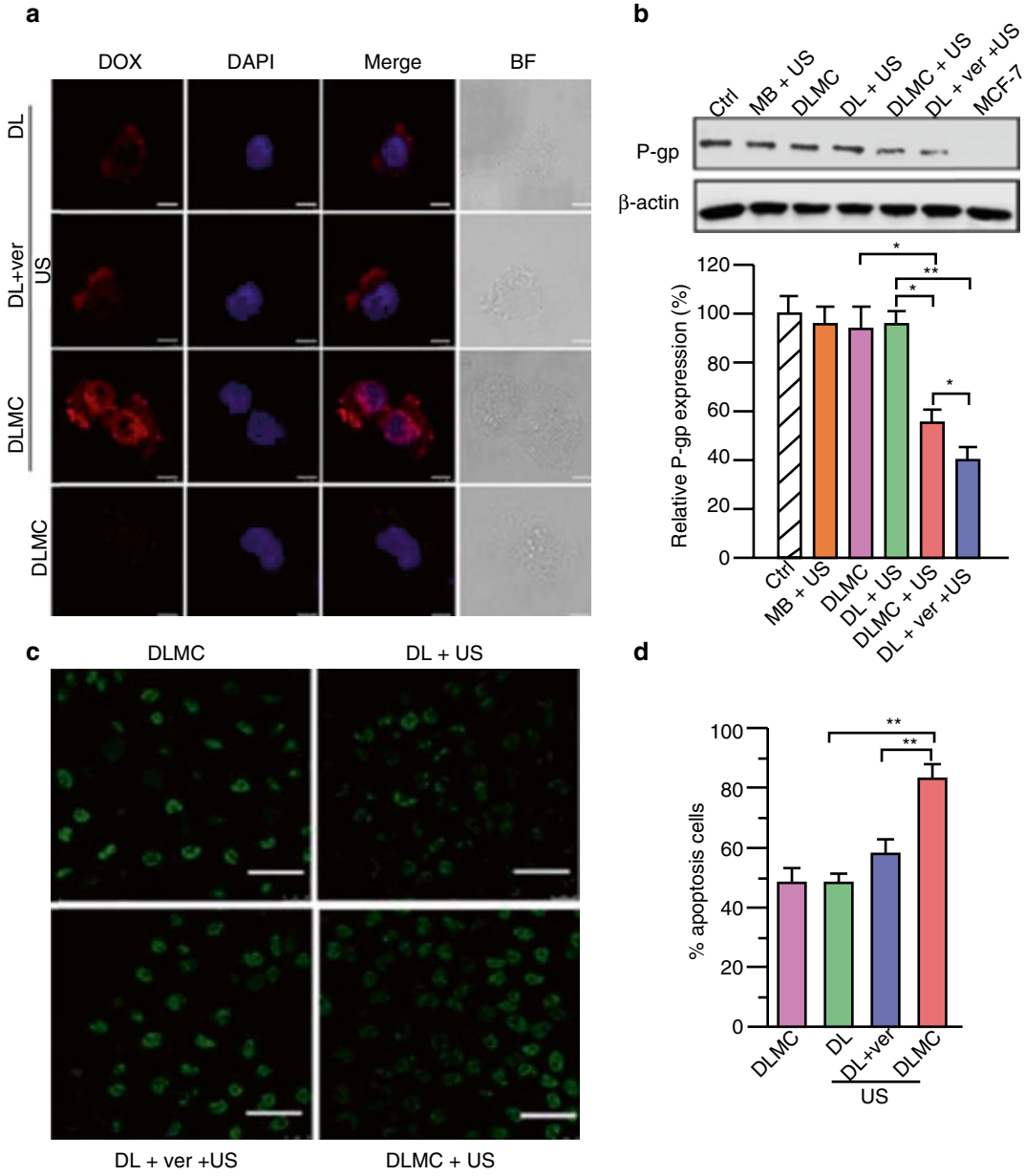

Fig. 15.6 Doxorubicin-resistant MCF-7 breast cancer cells were exposed to doxorubicin-liposome (DL)+ultrasound (US), DL+verapamil (ver) (a compound which reverses multidrug resistance by inhibiting drug efflux)+US, doxorubicin-liposome-microbubble complexes (DLMC)+US, and DLMC only. (a) Confocal microscopic images of intracellular doxorubicin distribution showed a more rapid cellular uptake and enhanced nuclear accumulation of doxorubicin using DLMC+US compared to other treatments. (b) Western-blotting showed down-regulated expression of P-glycoprotein using DLMC+US. (c) Apoptosis was detected by terminal deoxynucleotidyl transferase dUTP nick end labeling. (d) Quantitative analysis of apoptosis staining indicated significantly enhanced apoptosis using DLMC+US. *$p < 0.05$, **$p<0.01$ (This figure is adapted with permission from Deng et al. (2014))

drug efflux. Importantly, P-glycoprotein levels were substantially reduced in treated cells compared to non-treated cells (Fig. 15.6). Although the exact mechanism of reduced P-glycoprotein expression levels by USMB treatment remains unclear, it has been speculated that the

P-glycoprotein could have been mechanically removed from the cell membranes due to shear force induced by ultrasound-triggered microbubble cavitation (Brayman et al. 1999).

Alternatively, drug resistant tumors can be transfected with therapeutic genes to increase membrane transporters that shuffle drugs into tumor cells. This concept has been shown *in-vitro* in gemcitabine-resistant cells (dilazep-treated HEK293) transfected with human concentrative nucleoside transporter 3 (hCNT3) gene using USMB (Paproski et al. 2013). This resulted in a more than 2,000-fold increase of hCNT3 mRNA expression, and a subsequent more than 3,400-fold increased cellular uptake of gemcitabine relative to that in non-transfected cancer cells.

These two examples demonstrate that both physical impact of USMB on tumor cells and USMB-assisted transfection of transporter genes could potentially help overcome tumor cell drug resistance. However, so far experiments on this topic have only been performed under *in-vitro* conditions and further studies in animal models are warranted.

15.4.2 Adjuvant Treatment to Other Cancer Therapies

Adjuvant chemotherapy or radiotherapy is often applied following surgical resection in order to minimize local tumor recurrence and reduce tumor metastases. USMB-mediated drug delivery into a resection bed could become a part of a multimodality treatment approach of certain cancer types to reduce local recurrence rates. Sorace et al. (2014) proposed the use USMB-mediated delivery of cetuximab as adjuvant therapy following surgical resection of head and neck cancer in mice (1 MHz, 0.9 MPa peak negative pressure, 15 s pulse repetition period, 5 % duty cycle for 5 min). Tumors were resected at various degrees (0, 50, or 100 %), followed by adjuvant therapy with USMB-assisted delivery of cetuximab. During a 60-day post surgery observation period, there was no tumor recurrence in mice treated with complete tumor resection and USMB-aided drug treatment, while the recurrence rate was 66 % in animals receiving complete resection but no adjuvant USMB-guided therapy.

15.4.3 Cancer Vaccination

Cancer vaccination refers to the mediation that stimulates or restores the immune system's capability to treat existing cancer or prevent cancer development in certain high-risk individuals. The "classic" vaccine is currently achieved using tumor antigens isolated from surgical specimens or cancer cell lines, and made non-viable in *ex-vivo* conditions (Chiang et al. 2010). The non-viable antigens are then injected into the patient. The antigens can be taken up by the dendritic cells, processed intracellularly and subsequently expressed on the cell surface (Timmerman and Levy 1999). In the presence of antigen-presenting cells, the naïve T-cells are activated and play a central role in cell-mediated immunity to eliminate cancerous cells before they can do any harm. However, most clinical trials investigating cancer vaccination have failed or had very modest responses. A possible explanation is that the immune system of cancer patients is suppressed, with dendritic cells not recognizing the antigens to trigger an appropriate immune response in order to kill cancer cells.

USMB is currently being explored as a tool for *in-vivo* transfection of dendritic cells for cancer vaccination with improved transfection efficiency. It was found that antigen-encoding RNA intranodally injected into lymph nodes can be taken up by resident lymph node dendritic cells. Transfection of the dendritic cells propagated a T-cell attracting and stimulatory intralymphatic milieu, leading to efficient expansion of antigen-specific T cells, eliciting a protective and therapeutic anti-tumoral immune response (De Temmerman et al. 2011). The uptake of antigen-encoding RNA by dendritic cells could be further enhanced by the assistance of USMB. On the other hand, intradermally injected microbubbles can migrate to and successfully accumulate in lymph nodes (Sever et al. 2009). The accumulation of microbubbles can enhance

image contrast and facilitate *in-vivo* transfection of dendritic cells in the lymph nodes.

Oda et al. (2012) performed a first *in-vitro* proof-of-principle experiment and extracted tumor-specific antigens from melanoma cells. These were then delivered into dendritic cells with the assistance of USMB. This treatment induced 74.1 % of dendritic cells to present melanoma-derived antigens on their cell surface, relative to only 5.7 % in the group without USMB. These antigen-presenting dendritic cells were then intradermally injected twice into the backs of mice to assess effects in preventing melanoma lung metastases *in-vivo*. The results demonstrated a four-fold decrease in lung metastasis frequency after USMB-assisted prophylactic vaccination.

15.5 First Clinical Case Study

Recently, USMB was explored in a first clinical case study conducted by Kotopoulis et al. (Kotopoulis et al. 2013) in five patients with locally advanced pancreatic cancer. In this study, the patients were administered standardized gemcitabine treatment followed by sequential treatment with SonoVue® microbubbles and customized commercial ultrasound scanning over a period of 31.5 min (1.9 MHz, mechanical index 0.49, 1 % duty cycle, 5 kHz repetition rate, and 0.27 MPa peak negative pressure). The results showed that compared with a historical control group of 80 patients treated with gemcitabine alone, the 5 patients were able to tolerate a greater number of chemotherapy cycles (16 ± 7 *vs.* 9 ± 6 cycles). The tumor size was temporally or permanently reduced in 2 out of 5 patients, and the other 3 patients showed reduced tumor growth. No adverse effects related to this procedure were reported in this study.

This is the first report on sonoporation performed in a clinical setting, representing an important first step toward clinical development and hopefully also supporting subsequent clinical trials to be performed in additional institutions. However, this study has several limitations. Firstly, the treatment protocol has not been optimized, including ultrasound parameters and doses of drug and microbubbles. Future studies are warranted to explore this in the clinical setting. Secondly, only five patients were included for this pilot study and it remains unclear whether there was a true clinical benefit for the treated patients since there was no report on standard oncological outcomes, such as time to progression and overall survival time. Finally, long-term safety needs to be assessed for this treatment protocol.

An ongoing clinical trial conducted by the same research team including more patients with pancreatic cancer is expected to confirm this promising outcome (Helse Bergen and Georg 2010). Additionally, a clinical trial about the safety of USMB-assisted chemotherapy for the treatment of malignant neoplasms of the digestive system is currently being performed in China (Kun and Lin 2014). In this study, pancreatic cancer patients with liver metastases in whom routine chemotherapy has failed will be recruited. These patients will undergo treatment with USMB (SonoVue® microbubbles) and chemotherapy (platinum or gemcitabine). The tumor response rate and the safety limits on the mechanical index and ultrasound treatment time will be explored.

15.6 Prospects and Conclusions

Exciting results in preclinical studies and promising results in a first clinical case study show great potential for USMB-mediated drug delivery in cancer therapy. To further improve this technique and to develop it as a safe and efficient therapeutic approach, several issues need to be addressed.

15.6.1 Mechanisms of Microbubble-Tissue Interaction In-vivo

While multiple studies have provided some insight into the dynamic interaction between cavitating microbubbles and tumor cells for successful cellular drug delivery in a well-controlled *in-vitro* setup, successful drug delivery in an *in-vivo* environment is more complex and challenging. For a

drug to reach the target tumor cells *in-vivo*, several biological barriers have to be overcome. New insights into the mechanisms of sonoporation in *in-vivo* tumor tissue need to be further explored to allow optimal use of the biological implications of USMB-mediated drug delivery. The cavitation dynamics of microbubbles may be altered *in-vivo* compared to *in-vitro* settings due to the confinement from the surrounding tissues.

15.6.2 Advance in Multifunctional Microbubbles

Microbubbles play a key role in USMB-mediated drug delivery systems. Improved clinical outcomes may be achieved by the development of new microbubble formulations, with increased drug loading capacity and improved site-specific targeting. Several studies have been initiated towards these aims. For example, Borden et al. (2007) designed a multilayer construction using cationic polymers on the surface of positively charged microbubbles. These increased loading capacity of microbubbles for DNA by ten-fold. Covalently binding nanocarriers to microbubbles is an alternative approach, increasing loading capacity 34-fold without significantly increasing the diameter of the microbubble drug carrier (Sirsi and Borden 2014). In terms of further improvement of the targeting specificity, molecularly targeted microbubbles could be used that bind to markers differentially overexpressed on the tumor vasculature, such as VEGFR2, $\alpha_v\beta_3$ integrins or thymocyte differentiation antigen 1 (Lutz et al. 2014; Foygel et al. 2013; Bachawal et al. 2013; Wilson et al. 2013; Kircher and Willmann 2012a, b; Kiessling et al. 2012; Pysz and Willmann 2011; Deshpande et al. 2010; Schneider 2008).

15.6.3 Optimization of Drug Delivery Protocol

One of the main aims of USMB-mediated drug delivery research is to develop an optimal treatment protocol for improved drug delivery into tumor tissues. As mentioned above, several studies have investigated the influence of various ultrasound parameters, microbubble types and drug dosages, as well as routes of microbubble and drug administration, in order to identify more optimized settings for an USMB-assisted drug delivery approach. Unfortunately, so far, most optimization studies have been performed in cell culture experiments (Sonoda et al. 2007; Ghoshal et al. 2012), with only a few studies performed *in-vivo* (Sorace et al. 2012; Panje et al. 2012), these being limited to mouse tumor models. It is unclear whether these results obtained in mice are applicable in larger animals and even patients, where concerns of limited acoustic window and higher attenuation may arise for deeply seated tissues. Future research, systematically assessing the influences of various delivery parameters on the efficiency and safety of USMB-mediated drug delivery in larger animals is needed.

15.6.4 Development of a Dedicated Ultrasound System for Drug Delivery

USMB-mediated drug delivery can be achieved using clinical ultrasound imaging systems or custom-built ultrasound systems; however, limitations exist in both types of systems. The clinical imaging systems have very limited range of tunable pulse parameters and temporal pulsing sequences, which may result in less effective drug delivery outcomes. The custom-built ultrasound systems have more flexibility in pulse parameter and sequence design; however, these systems are usually assembled with a single element transducer. Mechanical motion of the transducer is often needed for a 3-dimensional raster scan over the entire tumor volume, which can be a time-consuming procedure. To address these issues, a more flexible system capable of generating a wide range of tunable pulse parameters and equipped with an array transducer capable of 3D electronic beam steering is essential. Development of a new system dedicated for drug delivery may substantially improve the therapeutic outcomes with minimally required treatment time.

15.6.5 Safety Studies

Although diagnostic ultrasound and contrast agents are considered safe and have been approved for use in clinical diagnostic imaging, safety of using ultrasound and microbubbles for therapeutic purposes needs to be systematically studied. A few preclinical studies in small animals so far have evaluated the safety of USMB using simple parameters, such as weight, eating habits and mobility (Pu et al. 2014; Kotopoulis et al. 2014; Zhou et al. 2010). However, more formal toxicity studies are likely required for various treatment protocols before clinical development.

Conclusions

The future success of cancer therapy is dependent on the development of noninvasive delivery methods that can efficiently and selectively deliver therapeutic agents to target cells with minimal systemic toxicity. Sonoporation, triggered by USMB, is a promising technique to fulfill this need. It is likely that drug delivery with USMB will benefit greatly from future improvements in molecular targeting strategies, engineering of new microbubble, and the development of precisely focusable ultrasound probes with optimized technical parameters of the ultrasound beam and optimized therapeutic temporal delivery sequences. This approach may provide much-needed therapeutic breakthroughs in cancer therapy, especially in cases where only palliative treatment is available.

References

Apfel RE, Holland CK (1991) Gauging the likelihood of cavitation from short-pulse, low-duty cycle diagnostic ultrasound. Ultrasound Med Biol 17:179–185

Bachawal SV, Jensen KC, Lutz AM, Gambhir SS, Tranquart F, Tian L, Willmann JK (2013) Earlier detection of breast cancer with ultrasound molecular imaging in a transgenic mouse model. Cancer Res 73:1689–1698

Bae YH (2009) Drug targeting and tumor heterogeneity. J Control Release 133:2–3

Bekeredjian R, Kroll RD, Fein E, Tinkov S, Coester C, Winter G, Katus HA, Kulaksiz H (2007) Ultrasound targeted microbubble destruction increases capillary permeability in hepatomas. Ultrasound Med Biol 33:1592–1598

Bohmer MR, Chlon CH, Raju BI, Chin CT, Shevchenko T, Klibanov AL (2010) Focused ultrasound and microbubbles for enhanced extravasation. J Control Release 148:18–24

Borden MA, Caskey CF, Little E, Gillies RJ, Ferrara KW (2007) DNA and polylysine adsorption and multilayer construction onto cationic lipid-coated microbubbles. Langmuir 23:9401–9408

Boucher Y, Baxter LT, Jain RK (1990) Interstitial pressure gradients in tissue-isolated and subcutaneous tumors: implications for therapy. Cancer Res 50:4478–4484

Brayman AA, Coppage ML, Vaidya S, Miller MW (1999) Transient poration and cell surface receptor removal from human lymphocytes in-vitro by 1 MHz ultrasound. Ultrasound Med Biol 25:999–1008

Carey LA, Perou CM, Livasy CA, Dressler LG, Cowan D, Conway K, Karaca G, Troester MA, Tse CK, Edmiston S, Deming SL, Geradts J, Cheang MC, Nielsen TO, Moorman PG, Earp HS, Millikan RC (2006) Race, breast cancer subtypes, and survival in the Carolina Breast Cancer Study. JAMA 295:2492–2502

Carlisle R, Choi J, Bazan-Peregrino M, Laga R, Subr V, Kostka L, Ulbrich K, Coussios CC, Seymour LW (2013) Enhanced tumor uptake and penetration of virotherapy using polymer stealthing and focused ultrasound. J Natl Cancer Inst 105:1701–1710

Carson AR, McTiernan CF, Lavery L, Grata M, Leng X, Wang J, Chen X, Villanueva FS (2012) Ultrasound-targeted microbubble destruction to deliver siRNA cancer therapy. Cancer Res 72:6191–6199

Caskey CF, Stieger SM, Qin S, Dayton PA, Ferrara KW (2007) Direct observations of ultrasound microbubble contrast agent interaction with the microvessel wall. J Acoust Soc Am 122:1191–1200

Chen H, Kreider W, Brayman AA, Bailey MR, Matula TJ (2011) Blood vessel deformations on microsecond time scales by ultrasonic cavitation. Phys Rev Lett 106:034301

Chiang CL, Benencia F, Coukos G (2010) Whole tumor antigen vaccines. Semin Immunol 22:132–143

Chuang YH, Wang YH, Chang TK, Lin CJ, Li PC (2014) Albumin acts like transforming growth factor beta1 in microbubble-based drug delivery. Ultrasound Med Biol 40:765–774

Cochran MC, Eisenbrey J, Ouma RO, Soulen M, Wheatley MA (2011a) Doxorubicin and paclitaxel loaded microbubbles for ultrasound triggered drug delivery. Int J Pharm 414:161–170

Cochran MC, Eisenbrey JR, Soulen MC, Schultz SM, Ouma RO, White SB, Furth EE, Wheatley MA (2011b) Disposition of ultrasound sensitive polymeric drug carrier in a rat hepatocellular carcinoma model. Acad Radiol 18:1341–1348

Davies Cde L, Lundstrom LM, Frengen J, Eikenes L, Bruland SO, Kaalhus O, Hjelstuen MH, Brekken C (2004) Radiation improves the distribution and uptake of liposomal doxorubicin (caelyx) in human osteosarcoma xenografts. Cancer Res 64:547–553

De Temmerman ML, Dewitte H, Vandenbroucke RE, Lucas B, Libert C, Demeester J, De Smedt SC, Lentacker I, Rejman J (2011) mRNA-Lipoplex loaded microbubble contrast agents for ultrasound-assisted transfection of dendritic cells. Biomaterials 32: 9128–9135

Deng Z, Yan F, Jin Q, Li F, Wu J, Liu X, Zheng H (2014) Reversal of multidrug resistance phenotype in human breast cancer cells using doxorubicin-liposome-microbubble complexes assisted by ultrasound. J Control Release 174:109–116

Deshpande N, Needles A, Willmann JK (2010) Molecular ultrasound imaging: current status and future directions. Clin Radiol 65:567–581

Dubinsky TJ, Cuevas C, Dighe MK, Kolokythas O, Hwang JH (2008) High-intensity focused ultrasound: current potential and oncologic applications. Am J Roentgenol 190:191–199

Ducreux M, Rougier P, Fandi A, Clavero-Fabri MC, Villing AL, Fassone F, Fandi L, Zarba J, Armand JP (1998) Effective treatment of advanced biliary tract carcinoma using 5-fluorouracil continuous infusion with cisplatin. Ann Oncol 9:653–656

Duvshani-Eshet M, Benny O, Morgenstern A, Machluf M (2007) Therapeutic ultrasound facilitates antiangiogenic gene delivery and inhibits prostate tumor growth. Mol Cancer Ther 6:2371–2382

Edelstein ML, Abedi MR, Wixon J (2007) Gene therapy clinical trials worldwide to 2007--an update. J Gene Med 9:833–842

Eggen S, Afadzi M, Nilssen EA, Haugstad SB, Angelsen B, Davies Cde L (2013) Ultrasound improves the uptake and distribution of liposomal Doxorubicin in prostate cancer xenografts. Ultrasound Med Biol 39:1255–1266

Eggen S, Fagerland SM, Morch Y, Hansen R, Sovik K, Berg S, Furu H, Bohn AD, Lilledahl MB, Angelsen A, Angelsen B, de Lange DC (2014) Ultrasound-enhanced drug delivery in prostate cancer xenografts by nanoparticles stabilizing microbubbles. J Control Release 187:39–49

Eikenes L, Bruland OS, Brekken C, Davies Cde L (2004) Collagenase increases the transcapillary pressure gradient and improves the uptake and distribution of monoclonal antibodies in human osteosarcoma xenografts. Cancer Res 64:4768–4773

Elodie Debefve YW, Krueger T, van den Bergh H (2013) Photodynamic therapy for increased delivery of anticancer drugs. In: Handbook of photomedicine. CRC Press, Florida

Fan Z, Liu H, Mayer M, Deng CX (2012) Spatiotemporally controlled single cell sonoporation. Proc Natl Acad Sci U S A 109:16486–16491

Ferlay J, Soerjomataram I, Ervik M, Dikshit R, Eser S, Mathers C, Rebelo M, Parkin DM, Forman D, Bray F (2014) Cancer worldwide. In: Stewart BW, Wild CP (eds) World cancer report 2014, vol 3. International Agency for Research on Cancer (IARC), Lyon, pp 16–80

Foygel K, Wang H, Machtaler S, Lutz AM, Chen R, Pysz M, Lowe AW, Tian L, Carrigan T, Brentnall TA, Willmann JK (2013) Detection of pancreatic ductal adenocarcinoma in mice by ultrasound imaging of thymocyte differentiation antigen 1. Gastroenterology 4:885–894

Fujii H, Matkar P, Liao C, Rudenko D, Lee PJ, Kuliszewski MA, Prud'homme GJ, Leong-Poi H (2013) Optimization of ultrasound-mediated anti-angiogenic cancer gene therapy. Mol Ther Nucleic Acids 2, e94

Fukumura D, Jain RK (2007) Tumor microenvironment abnormalities: causes, consequences, and strategies to normalize. J Cell Biochem 101:937–949

Ghoshal G, Swat S, Oelze ML (2012) Synergistic effects of ultrasound-activated microbubbles and doxorubicin on short-term survival of mouse mammary tumor cells. Ultrason Imaging 34:15–22

Goertz DE, Todorova M, Mortazavi O, Agache V, Chen B, Karshafian R, Hynynen K (2012) Antitumor effects of combining docetaxel (taxotere) with the antivascular action of ultrasound stimulated microbubbles. PLoS One 7, e52307

Gottesman MM (2002) Mechanisms of cancer drug resistance. Annu Rev Med 53:615–627

Greco A, Di Benedetto A, Howard CM, Kelly S, Nande R, Dementieva Y, Miranda M, Brunetti A, Salvatore M, Claudio L, Sarkar D, Dent P, Curiel DT, Fisher PB, Claudio PP (2010) Eradication of therapy-resistant human prostate tumors using an ultrasound-guided site-specific cancer terminator virus delivery approach. Mol Ther 18:295–306

Grossman R, Tyler B, Hwang L, Zadnik P, Lal B, Javaherian K, Brem H (2011) Improvement in the standard treatment for experimental glioma by fusing antibody Fc domain to endostatin. J Neurosurg 115: 1139–1146

Guarneri V, Dieci MV, Conte P (2012) Enhancing intracellular taxane delivery: current role and perspectives of nanoparticle albumin-bound paclitaxel in the treatment of advanced breast cancer. Expert Opin Pharmacother 13:395–406

Haag P, Frauscher F, Gradl J, Seitz A, Schafer G, Lindner JR, Klibanov AL, Bartsch G, Klocker H, Eder IE (2006) Microbubble-enhanced ultrasound to deliver an antisense oligodeoxynucleotide targeting the human androgen receptor into prostate tumours. J Steroid Biochem Mol Biol 102:103–113

Hauser J, Hauser M, Muhr G, Esenwein S (2009) Ultrasound-induced modifications of cytoskeletal components in osteoblast-like SAOS-2 cells. J Orthop Res 27:286–294

Heath CH, Sorace A, Knowles J, Rosenthal E, Hoyt K (2012) Microbubble therapy enhances anti-tumor properties of cisplatin and cetuximab in-vitro and in-vivo. Otolaryngol Head Neck Surg 146:938–945

Helse Bergen H, Georg D (2010) Treatment of pancreatic adenocarcinoma by combining contrast agent and gemcitabine under sonication. Helse Bergen HF, Haukeland Unversity Hospital, Bergen

Hobbs SK, Monsky WL, Yuan F, Roberts WG, Griffith L, Torchilin VP, Jain RK (1998) Regulation of transport pathways in tumor vessels: role of tumor type and

microenvironment. Proc Natl Acad Sci U S A 95: 4607–4612

Hoffmann A, Bredno J, Wendland M, Derugin N, Ohara P, Wintermark M (2011) High and low molecular weight fluorescein isothiocyanate (FITC)-dextrans to assess blood-brain barrier disruption: technical considerations. Transl Stroke Res 2:106–111

Iwanaga K, Tominaga K, Yamamoto K, Habu M, Maeda H, Akifusa S, Tsujisawa T, Okinaga T, Fukuda J, Nishihara T (2007) Local delivery system of cytotoxic agents to tumors by focused sonoporation. Cancer Gene Ther 14:354–363

Jain RK (1998) Delivery of molecular and cellular medicine to solid tumors. J Control Release 53:49–67

Jemal A, Bray F, Center MM, Ferlay J, Ward E, Forman D (2011) Global cancer statistics. CA Cancer J Clin 6:69–90

Juffermans LJ, Meijering BD, Henning RH, Deelman LE (2014) Ultrasound and microbubble-targeted delivery of small interfering RNA into primary endothelial cells is more effective than delivery of plasmid DNA. Ultrasound Med Biol 40:532–540

Kaneko OF, Willmann JK (2012) Ultrasound for molecular imaging and therapy in cancer. Quant Imaging Med Surg 2:87–97

Kiessling F, Fokong S, Koczera P, Lederle W, Lammers T (2012) Ultrasound microbubbles for molecular diagnosis, therapy, and theranostics. J Nucl Med 53:345–348

Kircher MF, Willmann JK (2012a) Molecular body imaging: MR imaging, CT, and US. Part I. Principles. Radiology 263:633–643

Kircher MF, Willmann JK (2012b) Molecular body imaging: MR imaging, CT, and US. Part II. Applications. Radiology 264:349–368

Kisker O, Becker CM, Prox D, Fannon M, D'Amato R, Flynn E, Fogler WE, Sim BK, Allred EN, Pirie-Shepherd SR, Folkman J (2001) Continuous administration of endostatin by intraperitoneally implanted osmotic pump improves the efficacy and potency of therapy in a mouse xenograft tumor model. Cancer Res 61:7669–7674

Kohane DS, Tse JY, Yeo Y, Padera R, Shubina M, Langer R (2006) Biodegradable polymeric microspheres and nanospheres for drug delivery in the peritoneum. J Biomed Mater Res A 77:351–361

Kotopoulis S, Dimcevski G, Gilja OH, Hoem D, Postema M (2013) Treatment of human pancreatic cancer using combined ultrasound, microbubbles, and gemcitabine: a clinical case study. Med Phys 40:072902

Kotopoulis S, Delalande A, Popa M, Mamaeva V, Dimcevski G, Gilja OH, Postema M, Gjertsen BT, McCormack E (2014) Sonoporation-enhanced chemotherapy significantly reduces primary tumour burden in an orthotopic pancreatic cancer xenograft. Mol Imaging Biol 16:53–62

Kun Y, Lin S (2014) Safety study of combining ultrasound microbubbles and chemotherapy to treat malignant neoplasms of liver metastases from gastrointestinal tumors and pancreatic carcinoma. Beijing Cancer Hospital, Beijing

Leslie TA, Kennedy JE (2006) High-intensity focused ultrasound principles, current uses, and potential for the future. Ultrasound Q 22:263–272

Liao ZK, Tsai KC, Wang HT, Tseng SH, Deng WP, Chen WS, Hwang LH (2012) Sonoporation-mediated anti-angiogenic gene transfer into muscle effectively regresses distant orthotopic tumors. Cancer Gene Ther 19:171–180

Liu HL, Hua MY, Chen PY, Chu PC, Pan CH, Yang HW, Huang CY, Wang JJ, Yen TC, Wei KC (2010) Blood-brain barrier disruption with focused ultrasound enhances delivery of chemotherapeutic drugs for glioblastoma treatment. Radiology 255:415–425

Lozano R, Naghavi M, Foreman K, Lim S, Shibuya K, Aboyans V, Abraham J, Adair T, Aggarwal R, Ahn SY, Alvarado M, Anderson HR, Anderson LM, Andrews KG, Atkinson C, Baddour LM, Barker-Collo S, Bartels DH, Bell ML, Benjamin EJ, Bennett D, Bhalla K, Bikbov B, Bin Abdulhak A, Birbeck G, Blyth F, Bolliger I, Boufous S, Bucello C, Burch M, Burney P, Carapetis J, Chen H, Chou D, Chugh SS, Coffeng LE, Colan SD, Colquhoun S, Colson KE, Condon J, Connor MD, Cooper LT, Corriere M, Cortinovis M, de Vaccaro KC, Couser W, Cowie BC, Criqui MH, Cross M, Dabhadkar KC, Dahodwala N, De Leo D, Degenhardt L, Delossantos A, Denenberg J, Des Jarlais DC, Dharmaratne SD, Dorsey ER, Driscoll T, Duber H, Ebel B, Erwin PJ, Espindola P, Ezzati M, Feigin V, Flaxman AD, Forouzanfar MH, Fowkes FG, Franklin R, Fransen M, Freeman MK, Gabriel SE, Gakidou E, Gaspari F, Gillum RF, Gonzalez-Medina D, Halasa YA, Haring D, Harrison JE, Havmoeller R, Hay RJ, Hoen B, Hotez PJ, Hoy D, Jacobsen KH, James SL, Jasrasaria R, Jayaraman S, Johns N, Karthikeyan G, Kassebaum N, Keren A, Khoo JP, Knowlton LM, Kobusingye O, Koranteng A, Krishnamurthi R, Lipnick M, Lipshultz SE, Ohno SL, Mabweijano J, MacIntyre MF, Mallinger L, March L, Marks GB, Marks R, Matsumori A, Matzopoulos R, Mayosi BM, McAnulty JH, McDermott MM, McGrath J, Mensah GA, Merriman TR, Michaud C, Miller M, Miller TR, Mock C, Mocumbi AO, Mokdad AA, Moran A, Mulholland K, Nair MN, Naldi L, Narayan KM, Nasseri K, Norman P, O'Donnell M, Omer SB, Ortblad K, Osborne R, Ozgediz D, Pahari B, Pandian JD, Rivero AP, Padilla RP, Perez-Ruiz F, Perico N, Phillips D, Pierce K, Pope CA 3rd, Porrini E, Pourmalek F, Raju M, Ranganathan D, Rehm JT, Rein DB, Remuzzi G, Rivara FP, Roberts T, De Leon FR, Rosenfeld LC, Rushton L, Sacco RL, Salomon JA, Sampson U, Sanman E, Schwebel DC, Segui-Gomez M, Shepard DS, Singh D, Singleton J, Sliwa K, Smith E, Steer A, Taylor JA, Thomas B, Tleyjeh IM, Towbin JA, Truelsen T, Undurraga EA, Venketasubramanian N, Vijayakumar L, Vos T, Wagner GR, Wang M, Wang W, Watt K, Weinstock MA, Weintraub R, Wilkinson JD, Woolf AD, Wulf S, Yeh PH, Yip P, Zabetian A, Zheng ZJ, Lopez AD, Murray CJ, AlMazroa MA, Memish ZA (2012) Global and regional mortality from 235 causes of death for 20 age groups in 1990

and 2010: a systematic analysis for the Global Burden of Disease Study 2010. Lancet 380:2095–2128

Lutz AM, Bachawal SV, Drescher CW, Pysz MA, Willmann JK, Gambhir SS (2014) Ultrasound molecular imaging in a human CD276 expression-modulated murine ovarian cancer model. Clin Cancer Res 5: 1313–1322

Markman M, Rowinsky E, Hakes T, Reichman B, Jones W, Lewis JL Jr, Rubin S, Curtin J, Barakat R, Phillips M et al (1992) Phase I trial of intraperitoneal taxol: a Gynecoloic Oncology Group study. J Clin Oncol 10: 1485–1491

Matsuo M, Yamaguchi K, Feril LB Jr, Endo H, Ogawa K, Tachibana K, Nakayama J (2011) Synergistic inhibition of malignant melanoma proliferation by melphalan combined with ultrasound and microbubbles. Ultrason Sonochem 18:1218–1224

Meijering BD, Juffermans LJ, van Wamel A, Henning RH, Zuhorn IS, Emmer M, Versteilen AM, Paulus WJ, van Gilst WH, Kooiman K, de Jong N, Musters RJ, Deelman LE, Kamp O (2009) Ultrasound and microbubble-targeted delivery of macromolecules is regulated by induction of endocytosis and pore formation. Circ Res 104:679–687

Minchinton AI, Tannock IF (2006) Drug penetration in solid tumours. Nat Rev Cancer 6:583–592

Molema G, Meijer DK, de Leij LF (1998) Tumor vasculature targeted therapies: getting the players organized. Biochem Pharmacol 55:1939–1945

Mow VC, Mak AF, Lai WM, Rosenberg LC, Tang LH (1984) Viscoelastic properties of proteoglycan subunits and aggregates in varying solution concentrations. J Biomech 17:325–338

Newman CM, Bettinger T (2007) Gene therapy progress and prospects: ultrasound for gene transfer. Gene Ther 14:465–475

Nie F, Xu HX, Lu MD, Wang Y, Tang Q (2008) Anti-angiogenic gene therapy for hepatocellular carcinoma mediated by microbubble-enhanced ultrasound exposure: an in-vivo experimental study. J Drug Target 16:389–395

O'Brien WD Jr (2007) Ultrasound-biophysics mechanisms. Prog Biophys Mol Biol 93:212–255

Oda Y, Suzuki R, Otake S, Nishiie N, Hirata K, Koshima R, Nomura T, Utoguchi N, Kudo N, Tachibana K, Maruyama K (2012) Prophylactic immunization with Bubble liposomes and ultrasound-treated dendritic cells provided a four-fold decrease in the frequency of melanoma lung metastasis. J Control Release 160:362–366

Panje CM, Wang DS, Pysz MA, Paulmurugan R, Ren Y, Tranquart F, Tian L, Willmann JK (2012) Ultrasound-mediated gene delivery with cationic versus neutral microbubbles: effect of DNA and microbubble dose on in-vivo transfection efficiency. Theranostics 2: 1078–1091

Panje CM, Wang DS, Willmann JK (2013) Ultrasound and microbubble-mediated gene delivery in cancer: progress and perspectives. Invest Radiol 48:755–769

Paproski RJ, Yao SY, Favis N, Evans D, Young JD, Cass CE, Zemp RJ (2013) Human concentrative nucleoside transporter 3 transfection with ultrasound and microbubbles in nucleoside transport deficient HEK293 cells greatly increases gemcitabine uptake. PLoS One 8, e56423

Park J, Zhang Y, Vykhodtseva N, Akula JD, McDannold NJ (2012a) Targeted and reversible blood-retinal barrier disruption via focused ultrasound and microbubbles. PLoS One 7, e42754

Park EJ, Zhang YZ, Vykhodtseva N, McDannold N (2012b) Ultrasound-mediated blood-brain/blood-tumor barrier disruption improves outcomes with trastuzumab in a breast cancer brain metastasis model. J Control Release 163:277–284

Parvizi J, Parpura V, Greenleaf JF, Bolander ME (2002) Calcium signaling is required for ultrasound-stimulated aggrecan synthesis by rat chondrocytes. J Orthop Res 20:51–57

Patil AV, Rychak JJ, Klibanov AL, Hossack JA (2011) Real-time technique for improving molecular imaging and guiding drug delivery in large blood vessels: in-vitro and ex vivo results. Mol Imaging 10:238–247

Pu C, Chang S, Sun J, Zhu S, Liu H, Zhu Y, Wang Z, Xu RX (2014) Ultrasound-mediated destruction of LHRHa-targeted and paclitaxel-loaded lipid microbubbles for the treatment of intraperitoneal ovarian cancer xenografts. Mol Pharm 11:49–58

Pysz MA, Willmann JK (2011) Targeted contrast-enhanced ultrasound: an emerging technology in abdominal and pelvic imaging. Gastroenterology 140:785–790

Qin S, Caskey CF, Ferrara KW (2009) Ultrasound contrast microbubbles in imaging and therapy: physical principles and engineering. Phys Med Biol 54:R27–R57

Rahman AM, Yusuf SW, Ewer MS (2007) Anthracycline-induced cardiotoxicity and the cardiac-sparing effect of liposomal formulation. Int J Nanomed 2:567–583

Schlicher RK, Radhakrishna H, Tolentino TP, Apkarian RP, Zarnitsyn V, Prausnitz MR (2006) Mechanism of intracellular delivery by acoustic cavitation. Ultrasound Med Biol 32:915–924

Schneider M (2008) Molecular imaging and ultrasound-assisted drug delivery. J Endourol 22:795–802

Sever A, Jones S, Cox K, Weeks J, Mills P, Jones P (2009) Preoperative localization of sentinel lymph nodes using intradermal microbubbles and contrast-enhanced ultrasonography in patients with breast cancer. Br J Surg 96:1295–1299

Sheikov N, McDannold N, Sharma S, Hynynen K (2008) Effect of focused ultrasound applied with an ultrasound contrast agent on the tight junctional integrity of the brain microvascular endothelium. Ultrasound Med Biol 34:1093–1104

Shillitoe EJ (2009) Gene therapy: the end of the rainbow? Head Neck Oncol 1:7

Sirsi SR, Borden MA (2014) State-of-the-art materials for ultrasound-triggered drug delivery. Adv Drug Deliv Rev 72:3–14

Sonoda S, Tachibana K, Uchino E, Yamashita T, Sakoda K, Sonoda KH, Hisatomi T, Izumi Y, Sakamoto T (2007) Inhibition of melanoma by ultrasound-microbubble-aided drug delivery suggests membrane permeabilization. Cancer Biol Ther 6:1276–1283

Sorace AG, Warram JM, Umphrey H, Hoyt K (2012) Microbubble-mediated ultrasonic techniques for

improved chemotherapeutic delivery in cancer. J Drug Target 20:43–54
Sorace AG, Korb M, Warram JM, Umphrey H, Zinn KR, Rosenthal E, Hoyt K (2014) Ultrasound-stimulated drug delivery for treatment of residual disease after incomplete resection of head and neck cancer. Ultrasound Med Biol 40:755–764
Suzuki R, Namai E, Oda Y, Nishiie N, Otake S, Koshima R, Hirata K, Taira Y, Utoguchi N, Negishi Y, Nakagawa S, Maruyama K (2010) Cancer gene therapy by IL-12 gene delivery using liposomal bubbles and tumoral ultrasound exposure. J Control Release 142:245–250
Szakacs G, Paterson JK, Ludwig JA, Booth-Genthe C, Gottesman MM (2006) Targeting multidrug resistance in cancer. Nat Rev Drug Discov 5:219–234
Taniyama Y, Tachibana K, Hiraoka K, Namba T, Yamasaki K, Hashiya N, Aoki M, Ogihara T, Yasufumi K, Morishita R (2002) Local delivery of plasmid DNA into rat carotid artery using ultrasound. Circulation 105:1233–1239
Timmerman JM, Levy R (1999) Dendritic cell vaccines for cancer immunotherapy. Annu Rev Med 50:507–529
Ting CY, Fan CH, Liu HL, Huang CY, Hsieh HY, Yen TC, Wei KC, Yeh CK (2012) Concurrent blood-brain barrier opening and local drug delivery using drug-carrying microbubbles and focused ultrasound for brain glioma treatment. Biomaterials 33:704–712
Todorova M, Agache V, Mortazavi O, Chen B, Karshafian R, Hynynen K, Man S, Kerbel RS, Goertz DE (2013) Antitumor effects of combining metronomic chemotherapy with the antivascular action of ultrasound stimulated microbubbles. Int J Cancer 132:2956–2966
Tong AW, Jay CM, Senzer N, Maples PB, Nemunaitis J (2009) Systemic therapeutic gene delivery for cancer: crafting Paris' arrow. Curr Gene Ther 9:45–60
Treat LH, McDannold N, Zhang Y, Vykhodtseva N, Hynynen K (2012) Improved anti-tumor effect of liposomal doxorubicin after targeted blood-brain barrier disruption by MRI-guided focused ultrasound in rat glioma. Ultrasound Med Biol 38:1716–1725
Tsai M, Lu Z, Wang J, Yeh TK, Wientjes MG, Au JL (2007) Effects of carrier on disposition and antitumor activity of intraperitoneal Paclitaxel. Pharm Res 24:1691–1701
Tzu-Yin W, Wilson KE, Machtaler S, Willmann JK (2014) Ultrasound and microbubble guided drug delivery: mechanistic understanding and clinical implications. Curr Pharm Biotechnol 14:743–752
van Wamel A, Bouakaz A, Versluis M, de Jong N (2004) Micromanipulation of endothelial cells: ultrasound-microbubble-cell interaction. Ultrasound Med Biol 30:1255–1258
van Wamel A, Kooiman K, Emmer M, ten Cate FJ, Versluis M, de Jong N (2006) Ultrasound microbubble induced endothelial cell permeability. J Control Release 116:e100–e102
Waite CL, Roth CM (2012) Nanoscale drug delivery systems for enhanced drug penetration into solid tumors: current progress and opportunities. Crit Rev Biomed Eng 40:21–41
Wang Y, Yuan F (2006) Delivery of viral vectors to tumor cells: extracellular transport, systemic distribution, and strategies for improvement. Ann Biomed Eng 34:114–127
Wang DS, Panje C, Pysz MA, Paulmurugan R, Rosenberg J, Gambhir SS, Schneider M, Willmann JK (2012) Cationic versus neutral microbubbles for ultrasound-mediated gene delivery in cancer. Radiology 264:721–732
Wang XL, Zhao XY, Li S, Jia CJ, Jiang L, Shi TM, Ren WD (2013a) A novel plasmid and SonoVue formulation plus ultrasound sonication for effective gene delivery in nude mice. Life Sci 93:536–542
Wang Y, Bai WK, Shen E, Hu B (2013b) Sonoporation by low-frequency and low-power ultrasound enhances chemotherapeutic efficacy in prostate cancer cells. Oncol Lett 6:495–498
Ward M, Wu J, Chiu JF (2000) Experimental study of the effects of optison concentration on sonoporation in-vitro. Ultrasound Med Biol 26:1169–1175
Willmann JK, van Bruggen N, Dinkelborg LM, Gambhir SS (2008) Molecular imaging in drug development. Nat Rev Drug Discov 7:591–607
Wilson KE, Wang TY, Willmann JK (2013) Acoustic and photoacoustic molecular imaging of cancer. J Nucl Med 54:1851–1854
Wood AK, Bunte RM, Price HE, Deitz MS, Tsai JH, Lee WM, Sehgal CM (2008) The disruption of murine tumor neovasculature by low-intensity ultrasound-comparison between 1- and 3-MHz sonication frequencies. Acad Radiol 15:1133–1141
Xing W, Gang WZ, Yong Z, Yi ZY, Shan XC, Tao RH (2008) Treatment of xenografted ovarian carcinoma using paclitaxel-loaded ultrasound microbubbles. Acad Radiol 15:1574–1579
Yamaguchi K, Feril LB Jr, Tachibana K, Takahashi A, Matsuo M, Endo H, Harada Y, Nakayama J (2011) Ultrasound-mediated interferon beta gene transfection inhibits growth of malignant melanoma. Biochem Biophys Res Commun 411:137–142
Yan F, Li L, Deng Z, Jin Q, Chen J, Yang W, Yeh CK, Wu J, Shandas R, Liu X, Zheng H (2013) Paclitaxel-liposome-microbubble complexes as ultrasound-triggered therapeutic drug delivery carriers. J Control Release 166(3):246–255
Yu BF, Wu J, Zhang Y, Sung HW, Xie J, Li RK (2013) Ultrasound-targeted HSVtk and Timp3 gene delivery for synergistically enhanced antitumor effects in hepatoma. Cancer Gene Ther 20:290–297
Zhang JZ, Saggar JK, Zhou ZL, Hu B (2012) Different effects of sonoporation on cell morphology and viability. Bosn J Basic Med Sci 12:64–68
Zhao YZ, Dai DD, Lu CT, Lv HF, Zhang Y, Li X, Li WF, Wu Y, Jiang L, Li XK, Huang PT, Chen LJ, Lin M (2012) Using acoustic cavitation to enhance chemotherapy of DOX liposomes: experiment in-vitro and in-vivo. Drug Dev Ind Pharm 38:1090–1098
Zhou S, Li S, Liu Z, Tang Y, Wang Z, Gong J, Liu C (2010) Ultrasound-targeted microbubble destruction mediated herpes simplex virus-thymidine kinase gene treats hepatoma in mice. J Exp Clin Cancer Res 29:170
Zimm S, Cleary SM, Lucas WE, Weiss RJ, Markman M, Andrews PA, Schiefer MA, Kim S, Horton C, Howell SB (1987) Phase I/pharmacokinetic study of intraperitoneal cisplatin and etoposide. Cancer Res 47:1712–1716